Preclinical investigation of potential new therapeutic targets in experimental cerebral large vessel occlusion

Doctoral thesis

Dr. Sándor Nardai

Semmelweis University

János Szentágothai Doctoral School of Neurosciences

Consultant supervisor: Dr. Zoltán Nagy, D.Sc. Professor emeritus

Dr. Judit Skopál, Ph.D. Senior research associate

Official reviewers: Dr. Eszter Farkas, Ph.D. Senior research associate

Dr. Tibor Kovács, Ph.D. Associate professor of neurology

Chairman of comprehensive examination committee:

Dr. Dániel Bereczki, D.Sc. Professor of neurology

Members of comprehensive examination committee:

Dr. János Martos, Ph.D., Department chief

Dr. Róbert Debreczeni, Ph.D., Adjunct lecturer

Budapest

2016

TABLE OF CONTENTS

ABBREVIATIONS

ACA	Anterior cerebral artery
AIF	Apoptosis-inducing factor
Ampa	D,L-α-amino-3-hydroxy-5-methyl-isoxazolpropionic acid
ASICs	Acid-sensing ion channels
BA	Basilary artery
BBB	Blood-brain barrier
Bcan	Brevican
Bdnf	Brain derived neurotrophic factor
CAP23	Membrane attached signal protein 1
Cat	Catalase
CBF	Cerebral blood flow
CI	Confidence intervall
C-jun	Jun proto-oncogene
CT	Computed tomography
CTA	Computed tomography angiography
Cuzd1	CUB and zona pellucida-like domains 1
Cxcl 12	Chemokine (C-X-C motif) ligand 12
CXCL8	C-X-C motif ligand 8
Cybb	Cytochrom b-245, beta polypeptide
Csnk2b	Casein kinase 2 beta
Cspg4	Chondroitin sulfate proteoglycan 4
DAB	3,3-diaminobenzidine
DAPT	Dual anti-platelet therapy
DCC	Deleted in colorectal carcinoma
DHC	Decompressive hemicraniectomy
DISC	Death inducing signaling complex
DQ gelatin	Dye-quenched gelatin
Egfr	Epidermal growth factor receptor
ELVO	Emergent large vessel occlusion
EphB1	Eph receptor B1
EU	European union
FADD	Fas associated death domain
Flt1	FMS-related tyrosine kinase
GAP 43	Growth associated protein 43
GAPDH	Glyceraldehid 3 phosphate dehydrogenase
Gpx1	Glutathion peroxidase 1
Hif1a	Hypoxia inducible factor 1, alpha subunit
IAT	Intra-arterial therapy
Iba1	Ionized calcium-binding adapter molecule 1
ICA	Internal carotid artery

Icam1	Intercellular adhesion molecule 1
ICH	Intra-cerebral hemorrhage
Igf1	Insulin-like growth factor 1
Igfbp6	Insulin-like growth factor binding protein 6
IL1$_\beta$	Interleukin 1 beta
Infg	Interferon gamma
IS	Ischemic stroke
Jag1	Jagged 1
Kdr	Kinase insert domain receptor
L1 cam	L1 cell adhesion molecule
LDF	Laser doppler flowmetry
Lingo 1	Leucine rich repeat and Ig domain containing 1
LOC	Level of consciousness
Lrp1	LDL receptor related protein 1
LVO	Large vessel occlusion
Mag	Myelin associated glycoprotein
MAO B	Monoamine oxidase B
Marcks	Myristoylated alanine rich protein kinase
MCA-M1	Middle Cerebral Artery proximal segment
MCA-M2	Middle Cerebral Artery first division side branch
Mmp12	Matrix metalloproteinase 12
Mmp2	Matrix metalloproteinase 2
Mmp9	Matrix metalloproteinase 9
Mog	Oligodendrocyte glycoprotein
MRI	Magnetic resonance imaging
mRNA	Messenger ribonucleic acid
mRS	Modified rankin scale
MTP	Mitochondrial transition pores
MWW	Mann-whitney-wilcoxon
Ncan	Neurocan
NCBI	National Center fo Biotechnology Information
nDNA	Nuclear deoxiribonucleic acid
NFM	Neurofilament N
Ngf	Nerve growth factor (beta polypeptide)
Ngfr (P75NTR)	Nerve growth factor receptor
NICD	Intracellular domain of Notch1
NIHSS	National Institute of Health Stroke Scale
NMDA	N-methyl-D-aspartate
Notch 1	Notch 1
Nogo receptor	Alternative name of the Reticulon 4 receptor
Nrp1	Neuropilin
NSA	Number of signal averages
Ntn 1	Netrin1

NVU	Neurovascular unit
P21	Cyclin dependent kinase inhibitor1a
PARP	Poly (ADP-ribose) polymerase
PCA	Posterior cerebral artery
PCR	Polimerase chain reaction
PirB	Paired Ig-like-receptor B
Plat	Plasminogen activator, tissue type
Ptprz1	Protein tyrosine phosphatase receptor Z1
Rac1	Ras-related botulinum toxin substrate 1
RCT	Randomized controlled trial
RECA	Rat endothelial cell antigen
ROS	Reactive oxigen species
Rtn4	Reticulon 4 (nogo a)
Rtn4r	Reticulon 4 receptor (Nogo receptor)
SAH	Subarachnoid hemorrhage
Sele	Selecin E
Sema3a	Semaphorin 3A
Sod1	Superoxide dismutase 1
Sod2	Superoxide dismutase 2
SPRR1	Small proline-rich protein 1
Stat3	Signal transducer and activator of transcription
TBST	Tris-buffer saline tween
TE	Echo time
TGF_{β} 1	Transforming growth factor, beta 1
TIA	Transient ischemic attack
TICI	Thrombolysis in Cerebral Infarction
TIMP1	Tissue inhibitor of metalloproteinase 1
TIMP2	Tissue inhibitor of metalloproteinase 2
TIMP3	Tissue inhibitor of metalloproteinase 3
TIMP4	Tissue inhibitor of metalloproteinase 4
tMCAO	Transient Middle Cerebral Artery Occlusion
Tnf	Tumor necrosis factor
TR	Repetition time
TTC	Tetraphyenil tetrazolium chloride
UV	Ultra violet
VA	Vertebral artery
Vcam1	Vascular cell adhesion molecule
Vcan	Versican
Vegfa	Vascular endothelial growth factor a
VISTA	Volume isotropic Turbo spin echo Acquisition
vWF	Von Willebrand factor

EXPERIMENTAL INVESTIGATION OF POTENTIAL NEW THERAPEUTIC TARGETS IN CEREBRAL LARGE VESSEL OCCLUSION

INTRODUCTION

Definitions

A stroke is the acute neurologic injury occurring as a result of brain ischemia or brain hemorrhage.

Brain ischemia is either due to thrombosis, embolism, or systemic hypoperfusion, while brain hemorrhages can be classified into intra-cerebral hemorrhage (ICH) and subarachnoid hemorrhage (SAH) (Caplan (2009).

Our current work focuses on the cerebral infarcts caused by emergent large vessel occlusions (ELVO). These ischemic strokes (IS) develop as a consequence of a proximal thrombotic blockage of the intra-cranial arteries, and their natural history is most often characterized by poor functional outcomes and high mortality rates (Lima et al., 2014).

While the findings of our preclinical investigations may have implications for other stroke subtypes, the transient middle cerebral artery occlusion (tMCAO) model used in our experiments most accurately simulates the pathophysiology of the ELVO, therefore we will limit our conclusions to this well-defined clinical entity. Chronic causes of intra-cranial large vessel occlusion, including Moya-Moya disease are beyond the scope of our dissertation due to their fundamentally different pathobiology.

Epidemiology of stroke and ELVO

Stroke is the second most common cause of mortality and the third most common cause of disability worldwide. The incidence rate of stroke is changing inversely in the high- and low-income countries, with an increasing incidence in the low-income group (Krishnamurthi et al., 2013) (Fig. 1.). While the overall rate of stroke-related mortality is decreasing worldwide, the absolute number of people with stroke, stroke survivors, stroke-related deaths, and the global burden of stroke-related disability is high and increasing (Feigin et al., 2014).

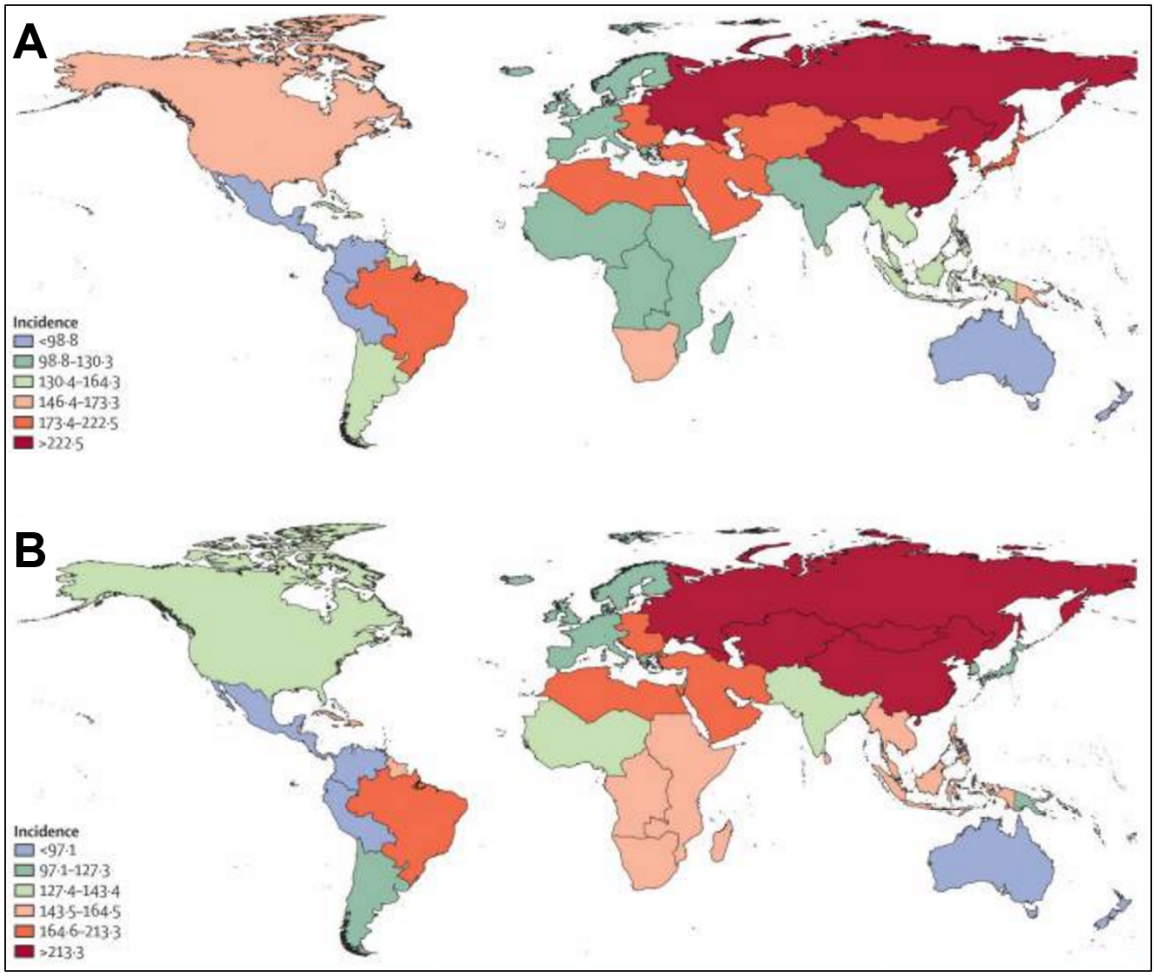

Figure 1. Age-standardized incidence of ischemic stroke per 100 000 person-years for 1990 (A) and 2010 (B). During the last 20 years incidence rates were changing in the opposite directions in the high- and low- income countries (Krishnamurthi et al., 2013).

Globally, the incidence of stroke due to ischemia is 68 percent, while the incidence of hemorrhagic stroke (ICH and SAH combined) is 32 percent, reflecting a higher incidence of hemorrhagic stroke in low- and middle-income countries (Krishnamurthi et al., 2013).

Following multiple imaging studies reporting a broad range of incidence rates, the first prospective registry evaluating the frequency of ELVO among all-comer patients admitted for thrombolysis work up was conducted in the Capital Region of Denmark between July 2009 and December 2011 (Hansen et al., 2015). Among the 885 patients evaluated for the suspicion of hyper-acute stroke within 4.5 h after symptom onset, computed tomography

angiogram (CTA) was performed in 637 subjects, including 475 patients with a final diagnosis of IS (74.6%) and 162 (25.4%) diagnosed with transient ischemic attack (TIA). The rest of the patients were excluded from analysis due to ICH (n=99), stroke mimics (n=147) or technical reasons (n=2). Altogether 28.7% (n=183) of the patient undergoing CTA had large vessel occlusion with 15 different anatomical distributions (Fig. 2). Based on these results more than one out of five patients evaluated for thrombolysis harbored ELVO. Important to note, that the majority of the large vessel occlusions involve the middle cerebral artery territory, confirming the adequacy of the tMCAO experiments for modelling this pathology.

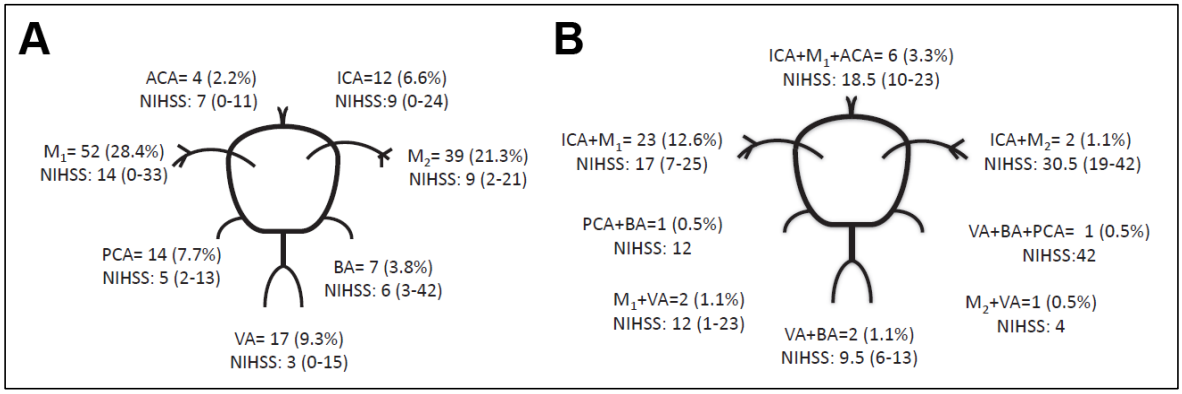

Figure 2. Anatomical distribution of large vessel occlusions. Number and % of patients with intra-cranial occlusions and their median National Institute of Health Stroke Scale (NIHSS) score in single vessel (A) and multiple vessel (B) disease. (Hansen et al., 2015)

Currently no epidemiologic data is available on the frequency of ELVO in Hungary. The country-specific figures published recently in the framework of the EuroHope Register however suggest a particularly high incidence of hospitalization (407/100000) and a high case fatality rate (31% at 1 year) of stroke among the Hungarian population compared to other studied European Union countries (Malmivaara et al., 2015). While the authors have raised some queries about the reliability of the administrative data derived from hospital discharges, a more severe initial presentation of the stroke cases together with a potentially higher frequency of ELVOs due to the lack of effective cardiovascular prevention may also be responsible for the documented excess mortality.

The natural history of ELVO

A proximal occlusions in the main intra-cranial arteries affect large brain territories by severely decreasing their perfusion. In a prospective registry of patients with untreated, unilateral ELVO of the anterior circulation, less than half of the observed subjects (44%) could achieve functional independence, and almost one-fourth (22%) of them were dead at 6 months. The only predictors for good functional outcome at 6 months were less severe neurological status (NIHSS<11) at presentation (see Appendix), younger age, and better collateral circulation (Lima et al., 2014).

The adverse outcomes associated with the ELVOs are not only the consequence of the extensive loss of functional neuronal circuits, but the larger infarct size itself is also an independent predictor of symptomatic hemorrhagic transformation, which leads to further neurological worsening and potentially excess mortality (Tan et al., 2014).

Another dreadful complication of the ELVOs is the malignant middle cerebral artery syndrome, which is characterized by a complete infarction of the MCA territory accompanied by the mass effect of a space occupying edema. The malignant evolution of the infarction develops within 5 days of symptoms onset, and it is associated with about 80% mortality if left untreated (Hacke et al., 1996). The early identification of patients who are most likely to develop malignant edema after MCA infarction is of paramount importance to plan the necessary interventions, including a timely performed decompressive hemi-craniectomy (DHC) if necessary.

Many clinical variables were proposed as surrogate markers for adverse evolution. A fairly low positive predictive value can be attributed to NIHSS >20, thrombus at the carotid terminus location, and early involvement of >50% of the MCA territory on native CT. Specificity is raised by the more precise volumetric analysis of the infarct size using MRI diffusion-weighted imaging: an infarct volume of >145cm^3 measured within 14 hours of symptom onset detected patients at high risk with 100% sensitivity and 94% specificity.

Based on the results of randomized trials, early DHC significantly reduces mortality after malignant MCA infarction; however, it also increases the probability of survival with moderately severe disability. The early timing of the surgery is crucial in achieving favorable outcomes, and it appears to benefit younger patients the most (Staykov and Gupta, 2011).

Reperfusion therapy in ELVO

Until very recently, intravenous alteplase administered within 4.5 hours after symptom onset was the only reperfusion therapy with proven efficacy in patients with acute IS (Emberson et al., 2014). Besides the broad range of contra-indications of this therapeutic modality, including coagulopathy, recent surgery and previous intra-cranial bleeding, systemic thrombolysis was proven to be much less effective in opening proximal occlusions. In the ELVO cases involving the ICA terminus the early recanalization rate was only about 30% using thrombolysis (Christou et al., 2001).

In 2015, five randomized clinical trials (Table 1) proved the higher efficacy of mechanical thrombectomy in the treatment of emergent LVOs compared to systemic thrombolysis, significantly changing the therapeutic recommendations for IS (Wahlgren et al., 2016). While the thorough presentation of these fundamental trials is beyond the scope of the thesis, some details are important to support the foundations of our experimental work.

Table 1. Recent randomized controlled trials of mechanical thrombectomy in LVO

Study name and reference	# of patients	**TICI 2b/3 flow**	Median NIHSS T/C	sICH % T/C	**Difference in good outcome***	Time from onset	**Onset to groin time**	Mortality % T/C
MR CLEAN *(Berkhemer et al., 2015)*	500	**59%**	17/18	7.7/6.4	**+14%**	<6h	**4h20m**	21/22
ESCAPE *(Goyal et al., 2015)*	316	72%	17/16	3.6/2.7	+24%	<12h	4h01m[a]	10/19
EXTEND-IA *(Campbell et al., 2015)*	70	**89%**	17/13	0/2.9	**+31%**	<6h	**3h30m**	9/20
SWIFT PRIME *(Saver et al., 2015)*	196	83%	17/17	0/3	+25%	<6h	4h12m	9/12
REVASCAT *(Jovin et al., 2015)*	206	66%	17/17	1.9/1.9	+16%	<8h	4h29m	18/16

Table 1. Selected date from the five recent RCTs on mechanical thrombectomy show that faster and more effective recanalization leads to better outcome. **Functionally independent patients (mRS 0-2 at three months) [a] Time to reperfusion.*

In contrast with the previous unsuccessful studies (Broderick et al., 2013; Kidwell et al., 2013), the new trials showing the improved functional outcomes associated with mechanical thrombectomy had some important common features. Only patients with confirmed large vessel occlusions were included, and the operators were able to rapidly achieve complete recanalization (TICI2b/3 flow) rate in a high proportion of the enrolled patients using the new generation stent retriever devices (Table 1). A recently published meta-analysis of the five trials showed similar positive results as the individual reports, and it also confirmed the efficacy of thrombectomy in patients who were not eligible for thrombolysis (Goyal et al., 2016) (Fig. 3, Table 2).

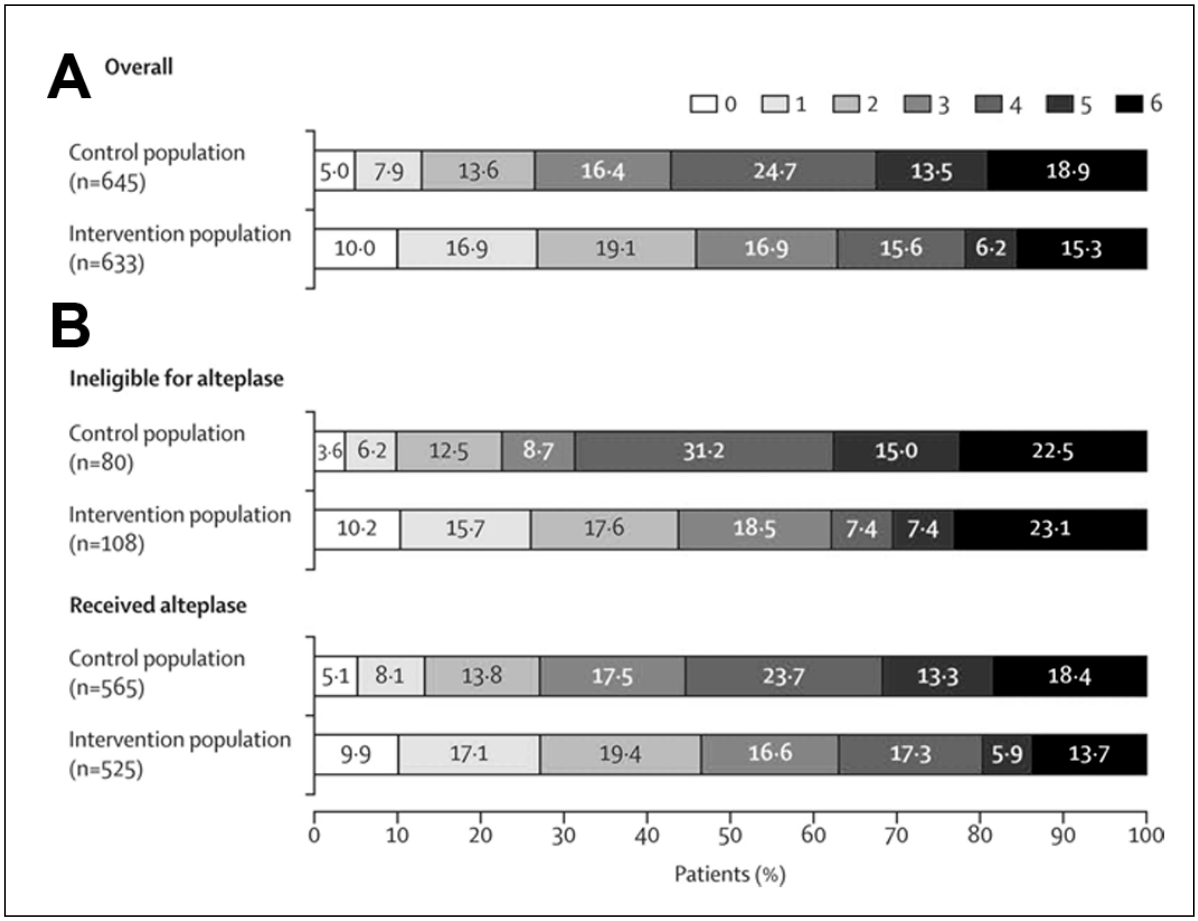

Figure 3. Functional outcomes of mechanical thrombectomy. Distribution of modified Rankin Scale scores at 90 days in the intervention and control groups in the overall trial population (A) and for patients treated with, or ineligible for intravenous alteplase (B). Data from the metaanalysis of the five RCTs (Goyal et al., 2016).

Table 2. Modified Rankin Scale (van Swieten et al., 1988)	
0	**No symptoms**.
1	**No significant disability**. Able to carry out all usual activities, despite some symptoms.
2	**Slight disability**. Able to look after own affairs without assistance, but unable to carry out all previous activities.
3	**Moderate disability**. Requires some help, but able to walk unassisted.
4	**Moderately severe disability**. Unable to attend to own bodily needs without assistance, and unable to walk unassisted.
5	**Severe disability**. Requires constant nursing care and attention, bedridden, incontinent.
6	**Dead**

Table 2. Standardized classification of functional outcomes following neurological injury according to Modified Rankin Scale (van Swieten et al., 1988).

The speed of recanalization is probably the most important factor determining the efficacy of thrombectomy (Fig. 3), as the amount of salvageable brain tissue and the chances of achieving good perfusion both steadily decrease with time. For every hour of reperfusion-delay, the initially large benefit of IAT decreases; the absolute risk difference for a good outcome is reduced by 6% per hour of delay (Fransen et al., 2016).

While the importance of optimizing the time window cannot be overemphasized, we have to keep in mind that some optimally chosen patients with good collaterals may also benefit from thrombectomy beyond 6 hours from the onset of symptoms (Goyal et al., 2015).

There is an ongoing debate over the optimal use of imaging modalities to select patients for mechanical reperfusion therapy, especially to identify potential candidates among the late presenters. CT based perfusion imaging (Campbell et al., 2015) and the imaging of collaterals (Goyal et al., 2015) were both used in the recent clinical trials, and with certain limitations, they both proved to be fairly accurate in guiding patient selection. Yet other authors claim that MRI may be the ideal modality (Wouters et al., 2016), as the DWI/perfusion mismatch clearly defines the unviable territory as well as the salvageable brain tissue. The optimal selections criteria for such patients is yet to be determined by further clinical research.

Safety issues of thrombectomy: prevention of bleeding complications and re-infarction

A very important aspect of the interventional treatment of ELVOs is the safety of the procedures. The analysis of the procedural complications did not show any excess bleeding or mortality associated with the more invasive interventional treatment (Table 3). We have to remember however, that the systemic thrombolysis alone already increases bleeding risk compared to the conservative management without reperfusion therapy, causing an average absolute increased risk of early death from ICH of about 2% (Emberson et al., 2014). Therefore further development is needed to prevent the reperfusion associated ICH, and the efficacy of thrombectomy alone in thrombolysis eligible patient should be also tested in new randomized controlled trails.

Table 3. Safety outcomes of the recent RCTs of mechanical thrombectomy at 90 days

	Interventional population	**Control population**	**Risk difference**	**Odds ratio (95% CI)**
Symptomatic ICH	**4.4% (28/634)**	**4.3%(28/653)**	**0.1 %**	**1.07 (0.62-1.83) p = 0.81**
Parenchymal hematoma type 2*	**5.1% (32/629)**	**5.3%(34/641)**	**-0.2%**	**0.99 (0.6-1.63) p = 0.97**
Mortality	**15.3% (97/633)**	**18.9%(122/646)**	**-3.6%**	**0.73 (0.47-1.13) p = 0.16**

Table 3. Meta-analysis of the safety outcomes of the five recent thrombectomy trials showed no risk difference between the treatment groups (Goyal et al., 2016) **Blood clot occupying >30% of the infarcted territory with substantial mass effect.*

The optimal estimation of the hemorrhagic and thrombotic risk of each individual patient is crucial for optimizing treatment outcomes. The actual stroke etiology as well as the extent of the brain damage has to be taken into account while determining the timing and composition of the antithrombotic regimen following cerebral large vessel recanalization. Evidence from a randomized trial confirms, that in the first 24 hours following treatment with intravenous alteplase, aspirin or other antithrombotic agent should not be given (Zinkstok and Roos, 2012). Afterwards the use of early aspirin (160 to 325 mg/day) rather than no aspirin therapy or early anticoagulation is recommended for most patients with acute ischemic stroke or TIA (Jauch et al., 2013; Lansberg et al., 2012). Early parenteral

anticoagulation rather than aspirin is only suggested for select patients with acute cardio-embolic ischemic stroke, who have a high suspicion for intracardiac thrombus, as these patients are at high risk for recurrent ischemic stroke. In atrial fibrillation, early therapeutic anticoagulation following acute stroke should be reserved to those harboring only minor intracerebral lesions based on control imaging, since in unselected patients the clinical benefit from the prevention of recurrent strokes was offset by the excess occurrence of intra-cranial bleeds (Sandercock et al., 2015).

Stroke patients presenting with significant intracranial large vessel stenosis represent a special subgroup, and according to recent evidence, they require early double anti-platelet therapy (DAPT) with the combination of aspirin and clopidogrel (Derdeyn et al., 2014). Patients receiving carotid stents as part of their acute stroke treatment also require DAPT after the exclusion of hemorrhagic transformation.

Important to note, that current antithrombotic strategies are mainly based on data from the old randomized trials of thrombolysis, therefore their validity following thrombectomy is not proven. Due to the fundamentally different recanalization efficacy and hemodynamic effect of the two reperfusion modalities, there is an urgent need for new RCTs in order to gather further evidence guiding the antithrombotic therapy following thrombectomy.

Another important, but currently less emphasized source of major complications in interventional stroke treatment is the access site bleeding. Due to the common co-occurrence of peripheral arterial disease and stroke, and the current therapeutic guidelines supporting the combined use of thrombolysis and thrombectomy, femoral artery punctures carry a non-negligible risk. Data from a recent metaanalysis comparing the safety of access sites in acute percutaneous coronary intervention show, that the use of radial artery can reduce vascular complication's rate and even mortality compared to femoral access (Ando and Capodanno, 2015). Our group has published a randomized trial comparing radial and femoral puncture during carotid artery stenting, and our results confirmed, that radial puncture allows efficient access for the treatment of vascular lesions of the neck in most cases (Ruzsa et al., 2014). Our findings also implicate, that radial approach may be used for thrombectomy in the future to avoid the complications associated with femoral puncture.

Potential adjunctive strategies to improve the functional outcomes of ELVO

The percutaneous revascularization of cerebral large vessel occlusions by mechanical thrombectomy is obviously a huge step forward in the optimal treatment of IS, and based on the above cited evidences the new therapeutic guidelines have given the highest level of recommendation for this treatment modality in eligible patients (Powers et al., 2015; Wahlgren et al., 2016). Ongoing clinical trials will help to further improve the patient selection in order to avoid the futile, and in some cases even harmful revascularizations. However there remains a large demand for the development of adjunctive therapies to offer alternative solutions to help the patients, who are non-eligible for reperfusion.

The infarcted brain tissue represents the common final stage of various different cascade mechanisms of cellular apoptosis and necrosis. The closely interrelated events occurring in the affected brain show a wide regional variety and diverse temporal pattern, making their investigation very challenging by conventional research methods. The system biology approach may provide a new insight into the pathophysiology of the brain vasculature (Clegg and Mac Gabhann, 2015), however the great amount of new information available at present time is not yet ready to formulate a new unifying concept for paving the foundations for new strategies of future stroke therapy.

Besides improving the outcomes with early reperfusion therapy, neuroprotective strategies or the effective augmentation of post-ischemic neuro-restorative mechanisms could be an alternative method to improve the prognosis of patients suffering from ELVO, however these approaches are still very far from being established treatment modalities. In order to find new therapeutic targets in stroke therapy, a fundamental understanding of the pathophysiology of ischemic brain lesions is crucial.

In the subsequent sections we will present the results of our recent investigations of two different pharmacological interventions, subacute gelatinase inhibition and selegiline treatment on a standard experimental model of ELVO in rodents. While the two treatments have been shown to inversely influence the functional outcomes after focal ischemia, their mechanism of action has not been fully explored before. We used an mRNA expression array analysis to study the effect of the interventions on the genes influencing post-stroke recovery.

Overview of the key regulatory genes influencing post-stroke recovery

The concept of the neurovascular unit (NVU) emphasizes the fact that neurons, astrocytes, smooth muscle cells, endothelial cells, pericytes, basement membranes, and the extracellular matrix all dynamically interact in the pathobiology of stroke (del Zoppo, 2009). The extent of recovery following brain injury is determined by the complex interplay of parallel processes involving the NVU, including synaptic and microvascular remodeling, inflammation, apoptosis, oxidative stress and structural alterations of the extracellular matrix. We sought to investigate the simultaneous changes induced by the two tested pharmacological interventions on the mRNA expression profile of the most important regulatory genes driving the remodeling processes of the penumbra. Despite the presentation of the key genes under distinct categories, it is important to keep in mind their redundancy, and their potential parallel regulatory roles.

Stroke induces a process of axonal sprouting in the peri-infarct tissue that results in a substantial re-mapping of the connections of the cortical areas adjacent to the infarct. This post-stroke axonal sprouting response is correlated in location and magnitude with functional recovery (Calautti and Baron, 2003). Nervous system injury induces expression of both growth-promoting and growth-inhibitory genes that together determine the location and degree of axonal sprouting.

The growth-promoting gene products (Table 4A) mediate growth cone membrane signaling events, transcriptional control in the regenerating neuron, cytoskeletal reorganization and axonal extension, and include GAP43, CAP23, MARCKS, c-jun, members of the stathmin family, Tα1 tubulin, L1, p21/waf1, and SPRR1. These proteins are specifically upregulated during sprouting, reduce axonal sprouting when knocked down or out, and mediate enhanced axonal sprouting when overexpressed (Benowitz et al., 2002; Bomze et al., 2001; Carmichael, 2003; Laux et al., 2000).

Stroke induces sequential waves of neuronal growth-promoting genes during the sprouting response: an early expression peak (SPRR1), a mid expression peak (p21, Ta1 tubulin, L1, MARCKS), a late peak (SCG10, SCLIP), and an early/sustained pattern (GAP43, c-jun). The expression of the growth inhibiting genes (Table 4B) show biphasic pattern. The growth-

inhibiting chondroitin sulfate proteoglycans aggrecan, brevican, versican, and phosphacan are induced late in the sprouting process; while the developmentally associated growth inhibitors ephrin-A5, ephB1, semaphorin IIIa, and neuropilin 1 are induced in the early phases of the sprouting response. At the cellular level, chondroitin sulfate proteoglycans are reduced in the region of axonal sprouting, during the peak of growth-promoting gene expression (Carmichael et al., 2005).

Table 4A Genes promoting axonal sprouting		
Abbreviation	**Name**	**NCBI Reference Sequence**
GAP 43	Growth associated protein 43	NM_017195.3
C-jun	Jun proto-oncogene	NM_021835.3
CAP23	Membrane attached signal protein 1	NM_022300.1
SPRR1	Small proline-rich protein 1	XM_574984.2
P21	Cyclin dependent kinase inhibitor1A	NM_080782.3
L1 cam	L1 cell adhesion molecule	NM_017345.1
Marcks	Myristoylated alanine rich protein kinase	XM_002728965.1
DCC	Deleted in colorectal carcinoma	NM_012841.1
Cuzd1	CUB and zona pellucida-like domains 1	NM_054005.1
NFM	Neurofilament N	NM_017029.1
Ntn 1	Netrin1	NM_053731.1
Table 4B Sprouting inhibitor genes		
Ncan	Neurocan	NM_031653.1
Vcan	Versican	NM_001170558.1
Ptprz1	Protein tyrosine phosphatase receptor Z1	NM_001170685.1
Cspg4	Chondroitin sulfate proteoglycan 4	NM_031022.1
Bcan	Brevican	NM_001033665.1
Sema3a	Semaphorin 3A	NM_017310.1
Nrp1	Neuropilin	NM_145098.2
EphB1	Eph receptor B1	NM_001104528.1
Rtn4	Reticulon 4 (Nogo A)	NM_031831.1
Rtn4r	Reticulon 4 receptor (Nogo receptor)	NM_053613.1
Ngfr (P75NTR)	Nerve growth factor receptor	NM_012610.2
Lingo 1	Leucine rich repeat and Ig domain containing 1	NM_001100722.1
Mag	Myelin associated glycoprotein	NM_017190.4
Mog	Oligodendrocyte glycoprotein	NM_022668.2
PirB	Paired Ig-like-receptor B	XM_001076302.2

Table 4. Genes promoting axonal sprouting (A) and sprouting inhibitors (B) included in the TaqMan® array analysis presented by the NCBI reference sequence, name and abbreviation.

The spatial and temporal dynamics of cerebral micro-vascular rearrangement after stroke are also closely related to neurological recovery. In a human post-mortem study sprouting angiogenesis was documented 5-92 days after stroke in the penumbra region (Krupinski et al., 1994). Scanning electron microscopic study of animal stroke models demonstrated, that radially arranged neocortical arterioles and small veins lost their regular patterns within one day of occlusion, and soon afterwards started to form a very dense network of anastomosing micro-vessels (Krupinski et al., 2003).

Compromised brain circulation activates complex processes that could facilitate the restoration of blood flow in the penumbra region. The low oxygen level prompts early response by activating oxygen responsive molecules, cytokines and other inflammatory factors (Table 5) (Beck and Plate, 2009). HIF-1a, the main regulator activates a series of genes responsible for metabolic changes in the penumbra, vasomotor tone and angiogenesis. Angiogenesis (sprouting or splitting and proliferating of endothelial cells in the preexisting blood vessel), vasculogenesis (de novo vessel growth) and arteriogenesis (transforming of small arteries into larger conducting arteries) result in neovascularization of the affected brain territory (Risau, 1997).

Table 5 Genes regulating microvascular remodeling

Abbreviation	**Name**	**NCBI Reference Sequence**
Vegfa	Vascular endothelial growth factor a	NM_001110333.1
Kdr	Kinase insert domain receptor	NM_013062.1
Flt1	FMS-related tyrosine kinase	NM_019306.1
Egfr	Epidermal growth factor receptor	NM_031507.1
Ngf	Nerve growth factor (beta polypeptide)	XM_227525.5
Bdnf	Brain derived neurotrophic factor	NM_012513.3
Igf1	Insulin-like growth factor 1	NM_001082477.2
Igfbp6	Insulin-like growth factor binding protein 6	NM_013104.2
Hif1a	Hypoxia inducible factor 1, alpha subunit	NM_024359.1
Notch 1	Notch 1	NM_001105721.1
Jag1	Jagged 1	NM_019147.1

Table 5. Genes promoting microvascular remodeling included in the TaqMan® array analysis presented by the NCBI reference sequence, name and abbreviation.

The reperfusion-mediated injury of the blood–brain barrier (BBB) is an important mechanism of the transformation from ischemic to hemorrhagic stroke. In addition to hemorrhage, a subset of patients do not improve after successful recanalization despite restored cerebral circulation (Dalkara and Arsava, 2012). Reperfusion injury is defined as a biochemical cascade causing a deterioration of ischemic brain tissue that parallels and antagonizes the beneficial effect of recanalization (Yang and Betz, 1994).

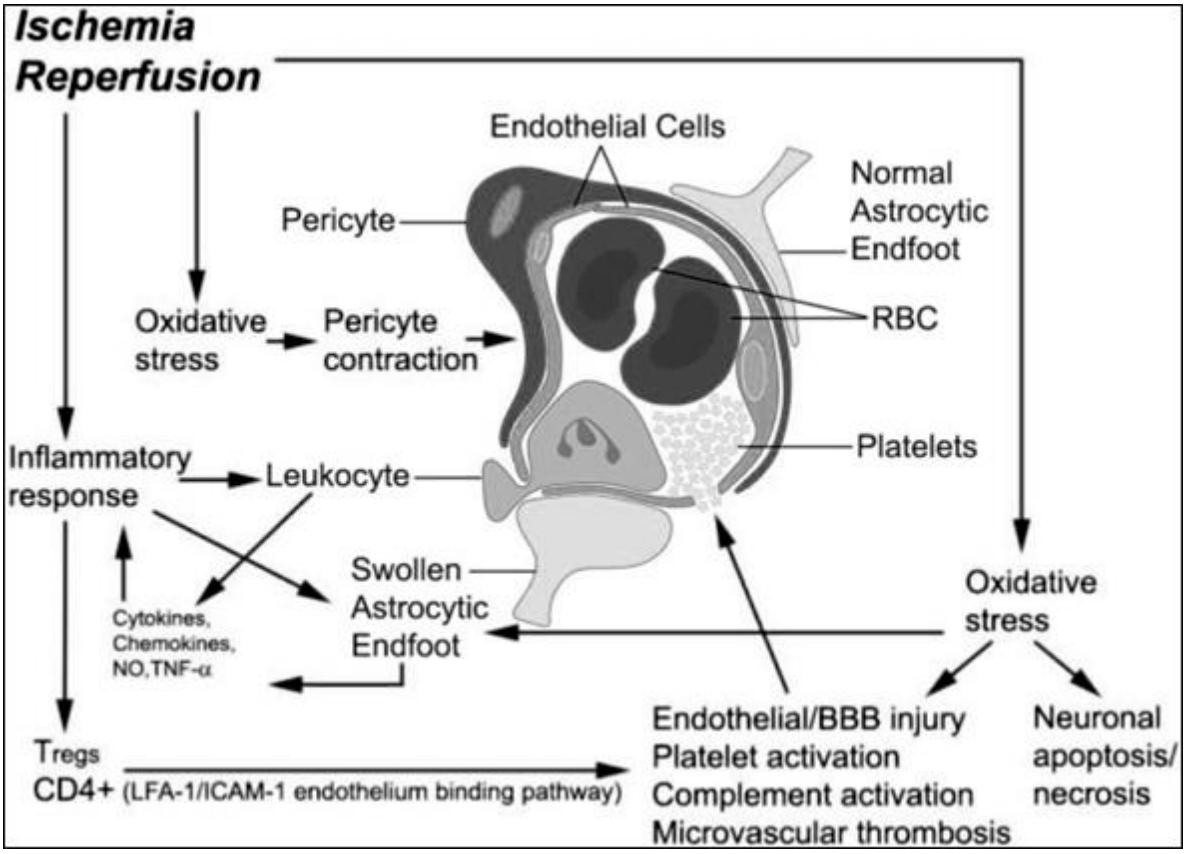

Figure 4. Schematic model of neurovascular mechanism of post-ischemic reperfusion injury. During reperfusion after ischemia, overproduction of reactive oxygen species (ROS) causes oxidative stress. The oxidative stress damages the endothelial cells, resulting in an exposure of the sub-endothelial extracellular matrix to blood flow. The exposure triggers adhesion and activation of platelets in microvasculature causing thrombosis. The injured endothelial cells release metalloproteinase that attacks basal lamina causing leakage of the blood–brain barrier (BBB)(Bai and Lyden, 2015).

Table 6 Genes involved in oxidative stress and reperfusion injury		
Abbreviation	**Name**	**NCBI Reference Sequence**
Cxcl 12	Chemokine (C-X-C motif) ligand 12	NM_001033882.1
$IL1_{\beta}$	Interleukin 1 beta	NM_031512.2
CXCL8	C-X-C motif ligand 8	NM_000584.3
Tnf	Tumor necrosis factor	NM_012675.3
Icam1	Intercellular adhesion molecule 1	NM_012967.1
Vcam1	Vascular cell adhesion molecule	NM_012889.1
Sele	Selecin E	NM_138879.1
TGF_{β} 1	Transforming growth factor, beta 1	NM_021578.2
Infg	Interferon gamma	NM_138880.2
Sod1	Superoxide dismutase 1	NM_017050.1
Sod2	Superoxide dismutase 2	NM_017051.2
Stat3	Signal transducer and activator of transcription	NM_012747.2
Csnk2b	Casein kinase 2 beta	NM_001035238.2
Cybb	Cytochrom b-245, beta polypeptide	NM_023965.1
Rac1	Ras-related botulinum toxin substrate 1	NM_134366.1
Gpx1	Glutathion peroxidase 1	NM_030826.3
Cat	Catalase	NM_012520.1
Mmp9	Matrix metalloproteinase 9	NM_031055.1
Mmp2	Matrix metalloproteinase 2	NM_031054.2
Mmp12	Matrix metalloproteinase 12	NM_053963.2
TIMP1	Tissue inhibitor of metalloproteinase 1	NM_053819.1
TIMP2	Tissue inhibitor of metalloproteinase 2	NM_021989.2
TIMP3	Tissue inhibitor of metalloproteinase 3	NM_012886.2
TIMP4	Tissue inhibitor of metalloproteinase 4	NM_001109393.1
Lrp1	LDL receptor related protein 1	NM_001130490.1
Plat	Plasminogen activator, tissue type	NM_013151.2

Table 6. Genes involved in the development of reperfusion injury included in the TaqMan® array analysis presented by the NCBI reference sequence, name and abbreviation.

During post-ischemic reperfusion in a focal transient MCAO rat model, BBB disruption is typically observed to be more severe than when compared with permanent MCAO. Furthermore, increased cerebral blood flow volume during reperfusion is correlated to worsened BBB disruption (Yang and Betz, 1994). Post-ischemic reperfusion causes enhanced production of free radicals and release of proteases from endothelial cells, astrocytes, microglia, and neurons. The matrix metalloproteinases (MMPs) play a major role mediating attack on the basal lamina in cerebral capillaries (Yang et al., 2007).

The core of brain tissue exposed to the most dramatic blood flow reduction is fatally injured and subsequently undergoes necrotic cell death within minutes of a focal ischemic stroke. A zone of less severely affected tissue around the necrotic core, also called as the "ischemic penumbra" is rendered functionally silent by reduced blood flow but remains metabolically active (Ginsberg, 1997). Many neurons in the penumbra region may undergo apoptosis after several hours or days, and thus they are potentially recoverable for some time after the onset of stroke. Apoptosis can be initiated by internal events (ie, "Intrinsic Pathway") (Fig. 5.) involving the disruption of mitochondria and the release of the cytochrome C, or alternatively, cell surface receptors can be activated by specific ligands that bind to "death receptors" (ie, "Extrinsic Pathway") (Fig. 6.) (Table 7A).

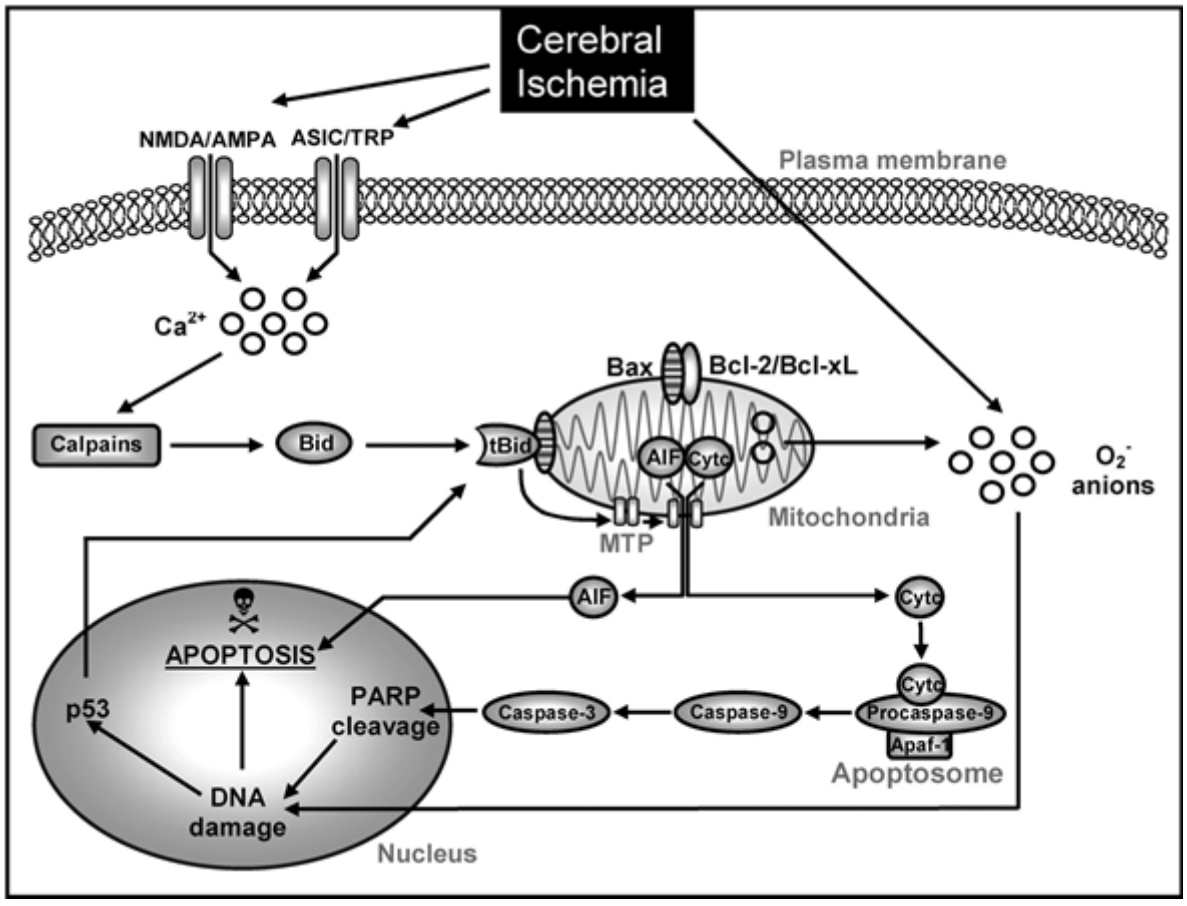

Figure 5. Intrinsic signaling of apoptosis in cerebral ischemia (Broughton et al., 2009)

Cerebral ischemia elevates cytosolic calcium levels through the stimulation by glutamate of N-methyl-D-aspartate (NMDA) or D,L-α-amino-3-hydroxy-5-methyl-isoxazolpropionic

acid (AMPA) receptors, or by the activation of acid-sensing ion channels (ASICs) . Increased intracellular calcium activates calpains and mediates cleavage of Bid to truncated Bid (tBid) initiating the intrinsic signaling cascade of apoptosis. At the mitochondrial membrane tBid interacts with apoptotic proteins such as Bad and Bax, which is typically neutralized by antiapoptotic B-cell leukemia/lymphoma 2 (Bcl-2) family proteins Bcl-2 or Bcl-xL. After heterodimerization of proapoptotic proteins with tBid, mitochondrial transition pores (MTP) are opened, thus releasing cytochrome c (Cytc) or apoptosis-inducing factor (AIF). Once released into the cytosol, Cytc binds with apoptotic protein-activating factor-1 (Apaf-1) and procaspase-9 to form an "apoptosome," which activates caspase-9 and subsequently caspase-3. Activated caspase-3 cleaves nDNA repair enzymes, such as poly (ADP-ribose) polymerase (PARP), which leads to nDNA damage and apoptosis. By contrast, AIF translocates rapidly to the nucleus where it mediates large-scale DNA fragmentation and cell death in a caspase-independent manner. In addition, nuclear pathways of neuronal apoptosis are activated in response to DNA damage, for example, through phosphorylation and activation of p53. Furthermore, cerebral ischemia and reperfusion generate superoxide anions ($O2^{-}$), which causes DNA damage (Broughton et al., 2009).

Extrinsic mechanisms of apoptosis involve the engagement of death receptors located on the plasma membrane and is hence also referred as the "death receptor pathway". Cell surface death receptors belong to the tumor necrosis factor receptor (TNFR) superfamily, and include TNFR-1, Fas, and $p75^{NTR}$.Forkhead1, a member of the forkhead family of transcription factors, stimulates expression of target genes, such as the Fas ligand (FasL) (Sugawara et al., 2004). The extracellular FasL binds to Fas death receptors (FasR), which triggers the recruitment of the Fas-associated death domain protein (FADD). FADD binds to procaspase-8 to create a death-inducing signaling complex (DISC), which activates caspase-8. Activated caspase-8 either mediates cleavage of Bid to truncated Bid (tBid), which integrates the different death pathways at the mitochondrial checkpoint of apoptosis, or directly activates caspase-3. At the mitochondrial membrane tBid interacts with Bax, which is usually neutralized by antiapoptotic B-cell leukemia/lymphoma 2 (Bcl-2) family proteins Bcl-2 or Bcl-xL. Dimerization of tBid and Bax leads to the opening of mitochondrial transition pores

(MTP), thereby releasing cytochrome c (Cytc), which execute caspase 3-dependent cell death (Broughton et al., 2009).

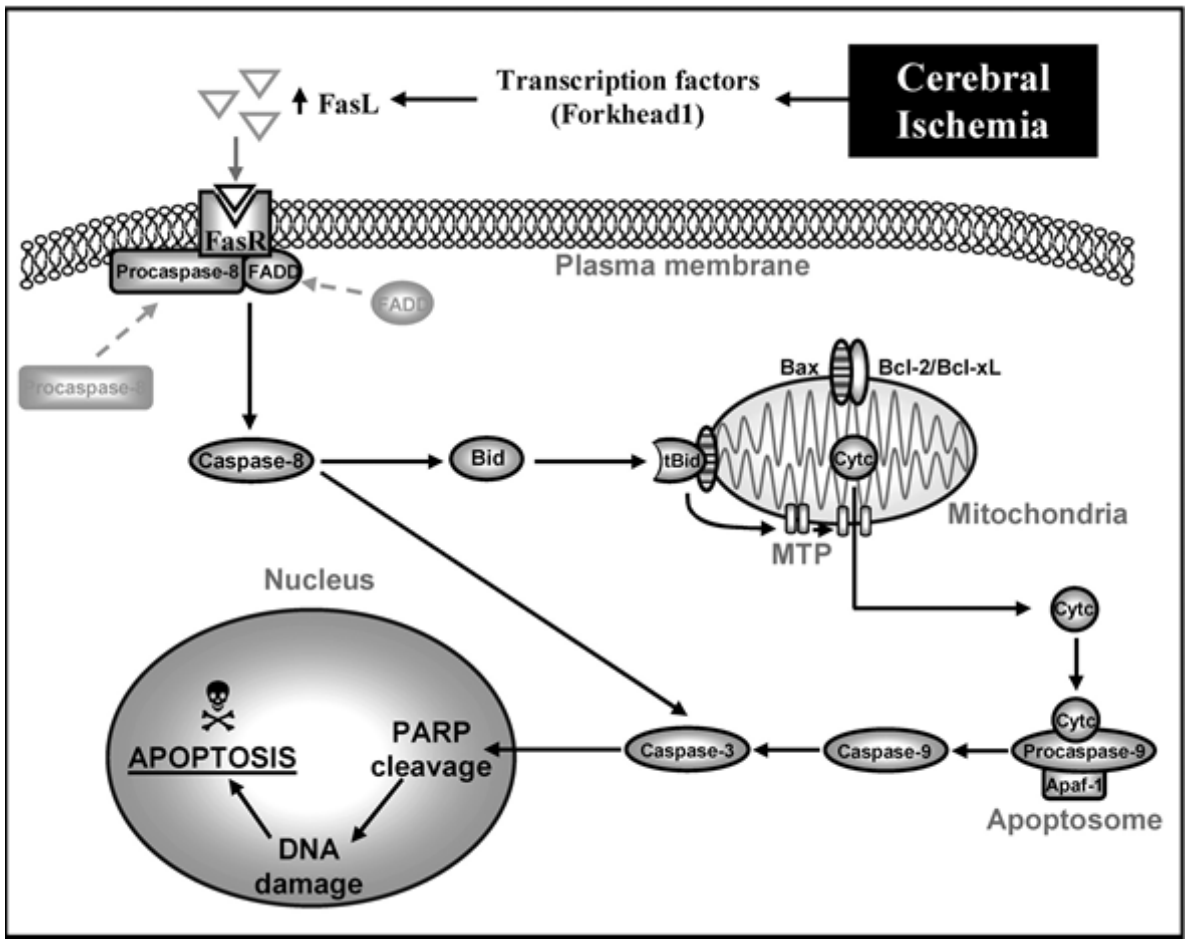

Figure 6. Extrinsic signaling of apoptosis after cerebral ischemia (Broughton et al., 2009)

Interactions between the pro-apoptotic and anti-apoptotic Bcl-2 family proteins on the outer mitochondrial membrane are believed to play an important role in cell survival (Love, 2003). Typically, anti-apoptotic members (Table 7B) are located on the outer membrane and suppress apoptosis through multiple mechanisms, including conserving mitochondrial membrane potential, inhibiting the release of apoptotic proteins, stabilizing the mitochondrial transition pores, thus preventing its opening, and controlling the activation of caspase proteases (Webster et al., 2006).

Table 7A Pro-apoptotic genes		
Abbreviation	**Name**	**NCBI Reference Sequence**
Bax	Bcl2-associated X	NM_017059.1
Bid	BH3 interacting domain death agonist	NM_022684.1
Casp1	Caspase 1	NM_012762.2
Casp2	Caspase 2	NM_022522.2
Casp3	Caspase 3	NM_012922.2
Casp6	Caspase 6	NM_031775.2
Casp7	Caspase 7	NM_022260.2
Casp8ap2	Caspase 8 associated protein 2	NM_001107921.1
Casp9	Caspase 9	NM_031632.1
Card 10	Caspase recruitment domain family	NM_001130554.1
Bcl2/11	Bcl2 like 11 transcript variant 1	NM_022612.1
Fadd	Fas associated via death domain	NM_152937.2
Apaf1	Apoptotic peptidase activating factor 1	NM_023979.1
Diablo	Diablo, IAP-binding mitochondrial protein	NM_001008292.1
Cycs	Cytochrome c	NM_012839.2
Bcl3	B-cell CLL/lymphoma 3	NM_001109422.1
Pidd1	P53-induced death domain protein 1	NM_001106318.2
Cradd	CASP2 and RIPK1 domain containing adaptor with death domain	NM_001108085.1
Table 7B Anti-apoptotic genes		
Abbreviation	**Name**	**NCBI Reference Sequence**
Proc	Protein c	NM_012803.1
Hspa1a	Heat shock 70kD protein 1A	NM_031971.2
Procr	Protein c receptor	NM_001025733.2
Fr2	Coagulation factor II receptor	NM_012950.2
Xiap	X-linked inhibitor of apoptosis	NM_022231.2
Ikbkg	Inhibitor of kappa light peptide gene enhancer in b-cells, kinase gamma	NM_199103.1
Nkap	NFKB activating protein	NM_001024872.1
Birc3	Baculovira IAP repeat containing 3	NM_023987.2
Naip	NLR family apoptosis inhibitor protein	XM_226742.4
Bcl2l2	Bcl2-like 2	NM_021850.2
Bcl2l1	Bcl2-like 1	NM_001033671.1
Ripk1	Receptor interactin serin/threonine kinase 1	NM_001107350.1

Table 7. Pro-apoptotic (A) and anti-apoptotic (B) genes included in the TaqMan® array analysis presented by the NCBI reference sequence, name and abbreviation.

AIMS:

Investigation of the molecular background of impaired recovery associated with gelatinase inhibition in the subacute phase of ELVO

The matrix metalloproteinase (MMP) 2 and 9 enzymes, also called as gelatinases (Fig. 7A), belong to the serine-protease enzyme family, and they are important factors in the hemorrhagic transformation of the ischemic brain lesions: they promote blood-brain barrier injury, and accelerate cerebral cell death (Asahi et al., 2001; Lee and Lo, 2004). Furthermore MMP 9 activity is enhanced by the thrombolytic agent used during reperfusion therapy (Burggraf et al., 2007), therefore the inhibition of MMP enzymes could be an ideal adjunctive treatment to prevent the hemorrhagic complications.

Contrary to their deleterious effect on acute lesions, gelatinases may mediate repair mechanisms during the delayed phases of stroke recovery. Pharmacological gelatinase inhibition 7 days after ischemic brain injury increased lesion size and impaired functional regeneration (Zhao et al., 2006).

Besides their proven interaction with neurovascular remodeling (Zhao et al., 2006), gelatinases may influence recovery through interaction with multiple growth promoting and inhibitory proteins. Gelatinase activity was demonstrated at the edge of the growth cone of dorsal root ganglion neurons (Hayashita-Kinoh et al., 2001), and the expression of phosphorylated neurofilament M, a marker for regenerative elongation, was induced by MMP9 (Demestre et al., 2004). Axonal re-myelination was also shown to require the proteolytic activity of the MMP9 (Oh et al., 1999), while the metalloproteinase mediated cleavage of the Reticulon 4 receptor (Rtn4r) was proposed as a potential disinhibitory mechanism that could enhance axonal regrowth (Walmsley et al., 2004). The same receptor was shown to mediate the astrocytic differentiation of neural progenitor cells, therefore the MMP-Rtn4r interaction may also influence the glial scar formation following central nervous system injury (Wang et al., 2008).

The aim of our study was to explore the molecular background of the impaired recovery associated with sub-acute metalloproteinase inhibition in ischemic stroke.

Investigation of the neuro-restorative action of Selegine in ELVO

Selegiline (Fig. 7B) is widely used in the therapy of Parkinson's disease (Tatton et al., 1994). Its effectiveness is based on the selective inhibition of monoamine oxidase B (MAO-B) and on its anti-apoptotic potential attributed to its ability to eliminate reactive oxygen species and stabilize mitochondrial membrane potential (Simon et al., 2005; Szilagyi et al., 2009).

In in vitro and animal studies our group has demonstrated previously that selegiline attenuates apoptosis and decreases infarct size after permanent occlusion of the middle cerebral artery (Simon et al., 2001). Furthermore, selegiline attenuated spatial learning deficits following focal cerebral ischemia in rats (Puurunen et al., 2001). The clinical use of the administration of low dose selegiline in the sub-acute phase of cerebral infarction has also been tested in a randomized, double-blinded, clinical pilot study. Although significant functional improvement was observed in stroke patients receiving selegiline in combination with physiotherapy, the molecular basis underlying this beneficial effect remained unclear (Sivenius et al., 2001). As the functional improvements were detected with the therapy being initiated days after the onset of stroke, the clinical efficacy was attributed to a potential neurorestorative rather than to the previously known neuroprotective properties of the molecule. This also means, that the selegiline treatment may potentially benefit those stroke patient who could not undergo reperfusion therapy as well.

To understand the mechanisms how selegiline exerts its actions following focal ischemia, we addressed its effects on gene expression.

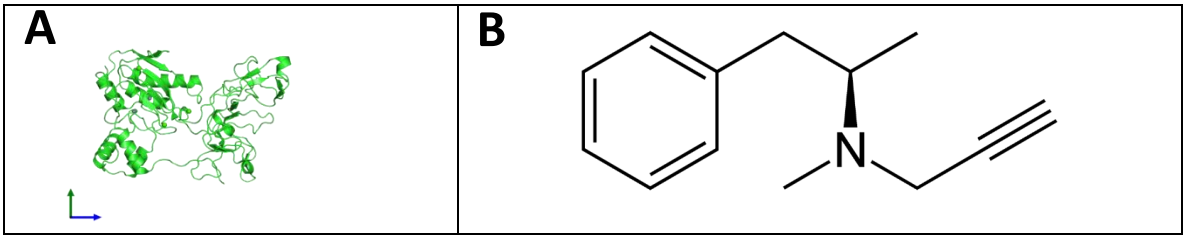

Figure 7. The crystal structure of the human Gelatinase B (Matrix Metalloproteinase 9) enzyme (A). (Elkins et al., 2002) and the structural formula of the (R) (-) deprenyl (Selegiline) molecule (B) (Knoll et al., 1978).

METHODS

The transient Middle Cerebral Artery Occlusion Model

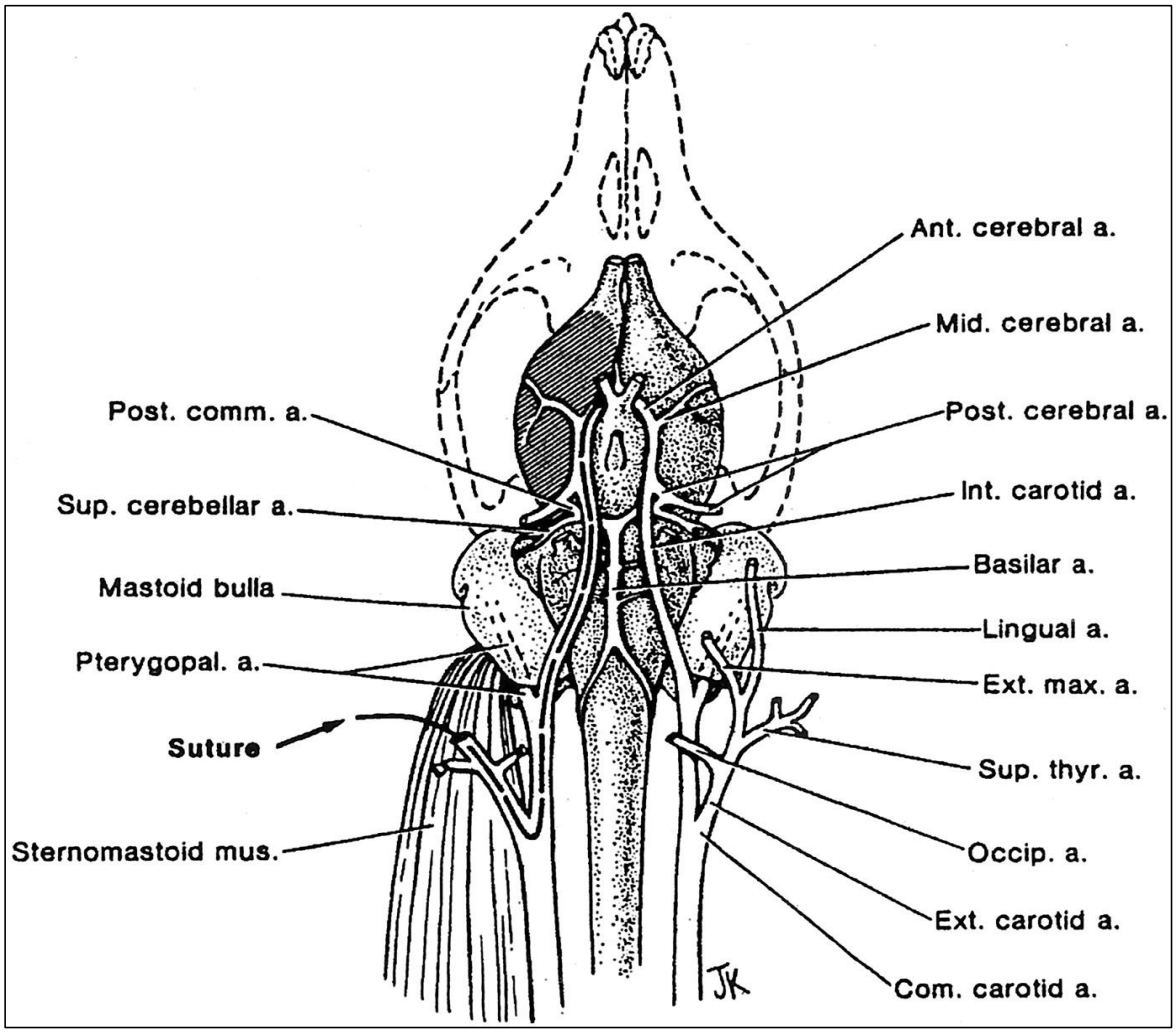

Figure 8. The MCAO filament technique. Schematic diagram displaying the rat carotid artery territories and the positioning of the MCAO filament (Longa et al., 1989).

The experimental model applied in our investigations to model the pathophysiology of thrombectomy in intra-cranial ELVO has been used for simulating stroke in rodents for decades (Longa et al., 1989). Important to note however, that the abrupt restoration of blood flow with the removal of the occluding filament simulate the hemodynamic changes associated with mechanical thrombectomy much better, than the hemodynamics of the gradual reperfusion occurring during thrombolysis.

Adult male CD rats (Charles River, Erkrath, Germany) were housed under controlled environmental conditions at an ambient temperature of 22°C with 12h light/dark cycle and free access to food and water. Brain ischemia was induced using slightly modified version of middle cerebral artery (MCA) filament occlusion model (Longa et al., 1989). Briefly, general anesthesia was induced using 5% isofluran in pure O_2 at 1 L/min for 4 min in male rats weighing 300-350 g. Animals were kept anaesthetized using 2% isoflurane in pure O_2 delivered by snout mask. Animal core (rectal) temperature was maintained constant at 37°C using temperature-controlled heat pad. A midline neck incision was made to expose the right carotid sheath under the operating microscope (Zeiss, Germany) The common carotid artery was isolated with 4-0 silk, and the occipital, pterygopalatine, and external carotid arteries were each isolated, cauterized, and divided. Right MCAO was accomplished by forming a small arteriotomy in the external carotid stump, and advancing a 25 mm 4-0 nylon suture with a 5 mm cast rubber tip (Doccol, Redlands, CA) through the arteriotomy into the internal carotid artery until the tip occluded the MCA (Fig 8.). To ensure adequate levels of cerebral ischemia, transcranial measurements of cerebral blood flow (CBF) were made over the MCA territory using Laser-Doppler Flowmetry (Perimed Inc., Stockholm, Sweden). Placement of the suture was confirmed by reduction of LDF readings to at least 40% of baseline (Fig. 9.). After 60 min of ischemia, animals were re-anesthetized and the occluding suture was removed.

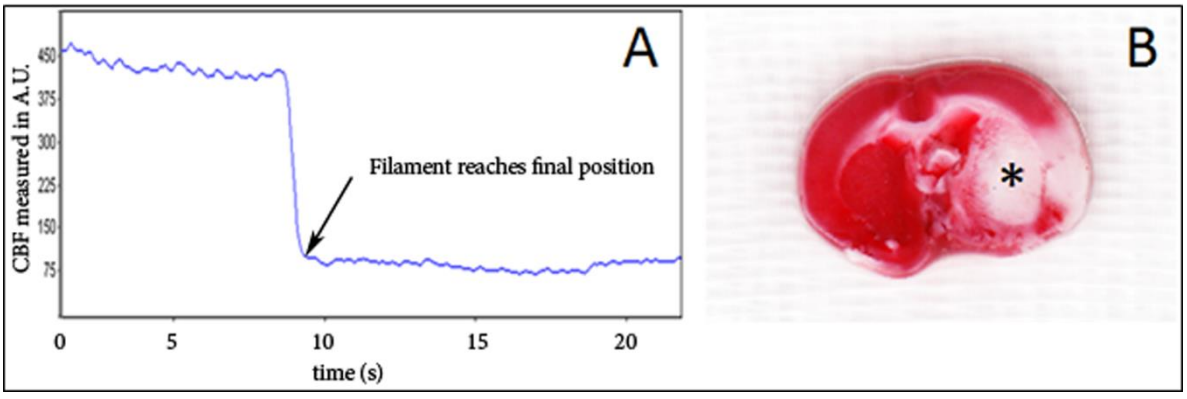

Figure 9. Trans-cranial measurements of the blood flow during tMCAO show a sudden drop in the cerebral perfusion at the time of the insertion of the occluding filament. (A). TTC staining of the native coronal brain section at bregma level delineates the ischemic lesion (*) by the lack of red staining of the viable mitochondria (B).

Stereotactic delivery of gelatinase inhibitor

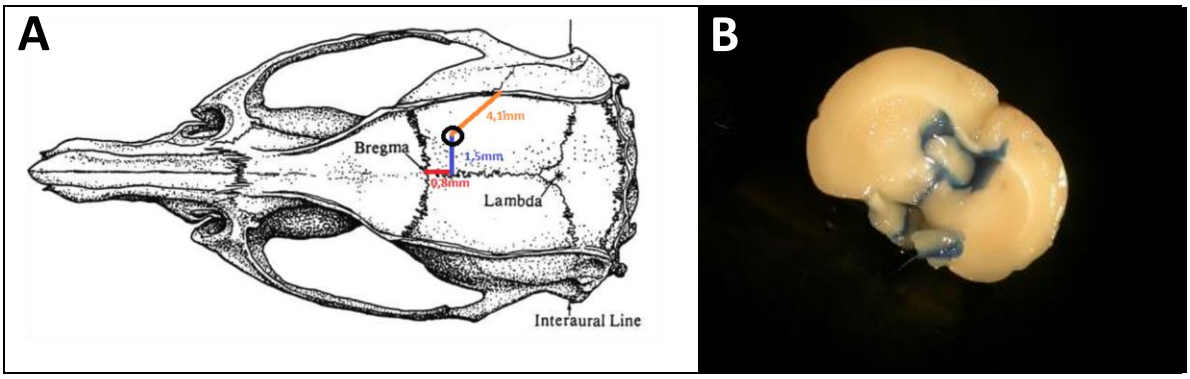

Figure 10. Stereotaxic injection for the delivery of the gelatinase inhibitor, rat specific coordinates: 0.8 mm caudal to Bregma, lateral: 1.6 mm to midline; depth: 4.1 mm to skull surface (A). Coronal section of a native rat brain demonstrating the successful stereotactic injection of Evans Blue dye into the right lateral ventricle (B).

Due to the excessive amount of inhibitor necessary for achieving sufficient gelatinase inhibitions intra-cranially with the currently available semi-selective compounds during systemic administration, we have decided to apply intra-cranial drug delivery using a dedicated stereotactic device. We performed pilot experiments on similar size rats (n=3) to ensure the adequate calibration of the stereotactic device (Harvard Apparatus, Boston, MA) using Evans Blue dye before applying the inhibitor treatments (Fig 10.) Finally 7 days after the tMCAO, we injected 20 µl of FN-439 metalloproteinase inhibitor (0.59 mg/kg, 720 mM in saline) or saline, into their right lateral ventricle of the animals over 20 min, using the previously calibrated stereotaxic injector under general anesthesia.

Administration of selegiline treatment

Selegiline treatment was started 48 hours following the initiation of the 60 min tMCAO. Animals in the treatment arm (n=6-6) were infused with 0.2 mg/kg/day of selegiline in a vehicle of 0.9% physiological saline, delivered *via* implantable osmotic pumps (Alzet, ALZA, Palo Alto, CA) placed intra-peritoneal for seven days (Fig. 11). Control rats (n=6-6) were infused with the vehicle only. The pumps were placed in the abdominal cavity under short general anesthesia. The rats were sacrificed after 7 days of treatment.

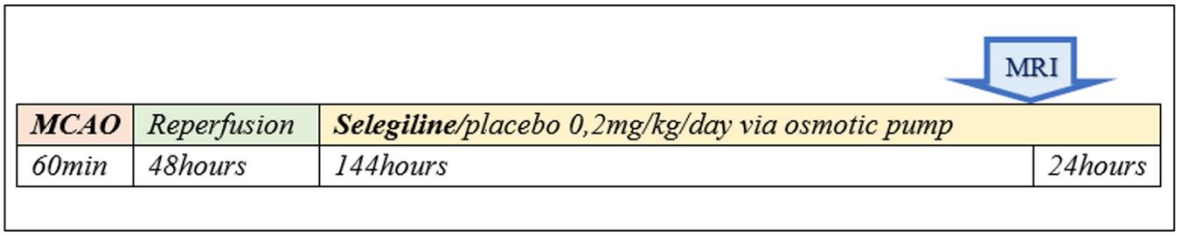

Figure 11. Experimental protocol of selegiline treatment. Continuous infusions were initiated 48 hours after MCAO. The animals underwent MRI investigation 24h before sacrifice.

Quantification of brain edema

Magnetic resonance imaging (MRI) study was performed on a 1.5 Tesla Philips Achieva clinical scanner using a SENSE-Flex-M coil 6 days after the initiation of treatment. After being anaesthetized with a bolus of ketamine/xilazin cocktail, animals were placed in supine position inside the clinical MRI scanner, and brain edema was visualized with a T2 weighted 3D VISTA sequence (Field of view: (AP/RL/FH) 60/60/45 mm, Voxel size: 0.6/0.6/1.2 mm, Reconstruction matrix = 128, number of slices =75, Echo time was set to the shortest possible, which resulted in TE=301 ms. Flip angle =90°; TR=2250 ms, NSA=5).

The obtained images were contrast enhanced to better differentiate edema from the background. Subsequently, planimetric measurements were performed on the coronal sections 7 mm posterior to the frontal pole using Image J software (NIH, Bethesda, USA). Animals with extensive cortical infarctions, potentially caused by failed reperfusion (1 animal in each group) were excluded from the statistical analysis.

The Animal Examination Ethical Council of the Animal Protection Advisory Board at the Semmelweis University, Budapest specifically approved these studies. Thus, the procedures involving rats were carried out according to experimental protocols that meet the guidelines of the Animal Hygiene and Food Control Department, Ministry of Agriculture, Hungary, which is in accordance with EU Directive 2010/63/EU for animal experiments EU Directive 2010/63/EU for animal experiments.

The animal experiments were carried out at the Experimental laboratory of the Heart and Vascular Center of Semmelweis University, and the imaging studies were done at the MRI Unit of the Heart and Vascular Center.

Tissue sampling and mRNA extraction for the TaqMan® array analysis

Nine days after the tMCAO, the animals were decapitated and their brains were rapidly removed. Coronal sections (12 μm thick) were cut from the native brain tissue using a rat brain matrix (Harvard Apparatus, Boston, USA) starting 6 mm caudal to the frontal pole. Tetraphenyl-tetrazolium chloride (TTC) staining was performed on the first coronal sections (6-8 mm from the frontal pole of the brain) to identify the lesion. After 15 min of incubation at 37°C, 3 samples of brain tissue from the border of the ischemic lesion were dissected using a 2 mm diameter punch biopsy needle. Total RNA was extracted with TRIzol reagent (Invitrogen, Carlsbad, CA) according to the manufacturer's instructions. The extracted RNA was quantified using UV spectrophotometry; only samples with a 260:280 ratio greater than 1.7 were further processed (Fig 12.). RNA was reverse transcribed in duplicates using Omniscript kit (Qiagen, Valencia, CA). A third RNA sample was incubated without reverse transcriptase as a no-RT control.

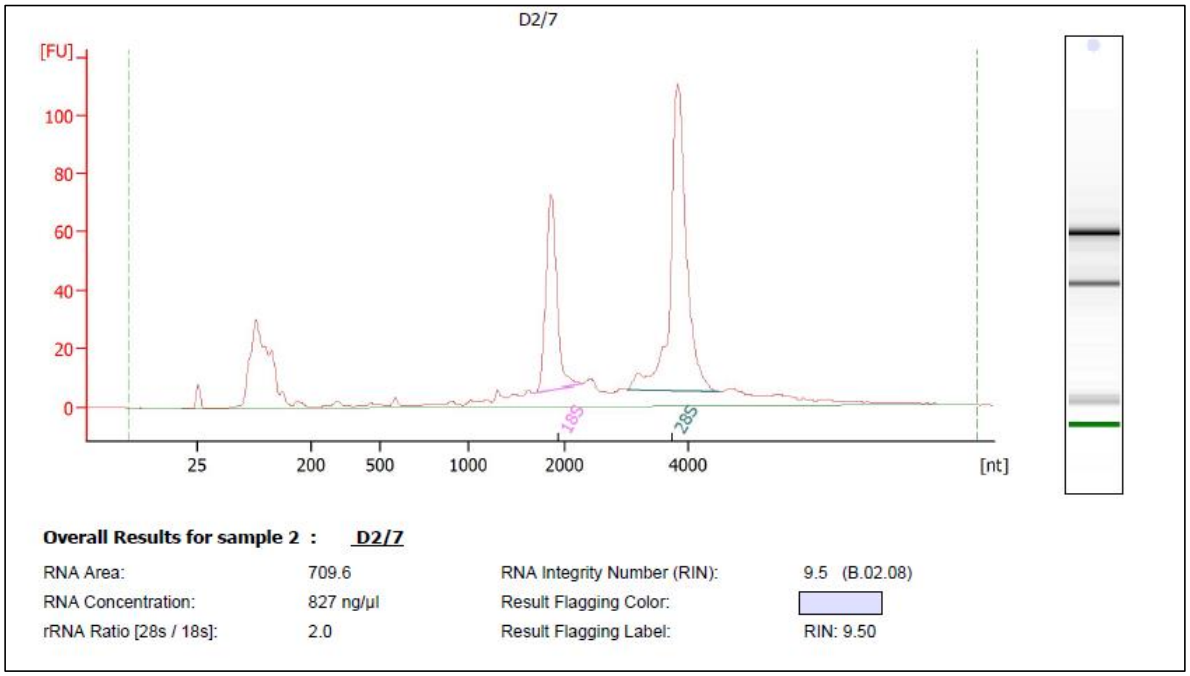

Figure 12. UV spectrophotometry analysis of a good quality total RNA sample with a 28s/18s RNA ratio > 1,7.

TaqMan® array analysis

Samples were run parallel on a custom designed TaqMan® gene expression array containing probes for 84 representative genes involved in axonal sprouting, apoptosis regulation, reperfusion injury and neurovascular remodeling based on literature data (See Table 4-7). Gene expressional values were compared between the treatment and control groups after being normalized to a previously established housekeeping control (Psmc4-Rn00821605_g1). Initially 4 housekeeping controls were tested, and the one with the most table expression pattern was chosen for reference. We have only evaluated those probes in the final analysis, that were adequately functioning in both parallel samples of all included subjects (n=5+5 for the gelatinase inhibitor and n=6+6 for selegiline respectively).

RNA isolation and Real-Time Quantitative PCR measurement was performed by UD-GenoMed Medical Genomic Technologies Ltd (Debrecen, Hungary).

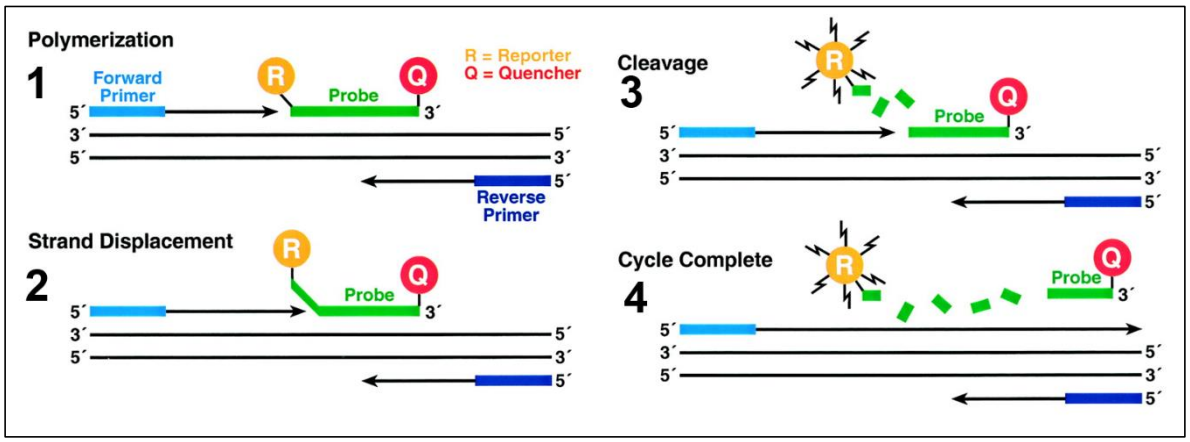

Figure 13. Schematic of the TaqMan principle. Polymerization catalyzed by the Taq enzyme proceeds as typical for a PCR reaction using forward and reverse primers. Allele-specific fluorogenic probes, 5′ labeled with a reporter dye and 3′ labeled with a quencher dye, hybridize to complementary templates (1-2). Proximity of the two dyes allows the quencher dye to absorb the emission of the reporter dye. During polymerization, the Taq enzyme displaces and cleaves hybridized probes (3-4), producing an exponential increase in cleaved reporter dye emission. TaqMan probes were named after the videogame Pac-Man (*Taq* Polymerase + PacMan = TaqMan) as its mechanism is based on the Pac-Man principle (Yuan et al., 2000).

In situ gelatin zymography

Successful inhibition of the MMP activity was demonstrated by in situ gelatin zymography. The frontal part of the brain was cut into 20μm thick slices, and the samples were incubated overnight at 37°C with 40μl/ml DQ gelatin-FITC (Molecular Probes, Eugene, OR) (Amantea et al., 2008). After washing away the excess gelatin, the slides were cover slipped. 5 fields of view were captured in the peri-infarct cortex through a fluorescent microscope (Zeiss, Germany) to be analyzed with the Image J software (NIH, Bethesda, DC).

Antibody selection and tissue preparation for immunolabeling

The information gathered from our array analysis largely resembles of looking for something very small in a large mist at night using a very dime flashlight. Some silhouettes can be made out, but further definition of the objects is definitely needed by another modality. Immunolabeling, if feasible, is a very reliable method for confirming our initial findings and to localize the protein end-products of the upregulated genes. However the considerable damage to the brain tissue make this technic challenging in the context of experimental stroke, therefore we have limited the use of this rather time consuming modality to study the most relevant gene expressional changes found in our array experiments. We have performed immunolabeling for the intracellular domain of Notch1 (NICD), Jagged 1 and we used (rat endothelial cell antigen) RECA antibodies to analyze micro-vessel density in the Selegiline study. In the MMP inhibitor experiments we applied the Reticulon 4 receptor (Rtn4r) antibody. We also performed double-labeling using standard cellular markers. (See below).

After several attempts to optimize the quality of the labeling, we have decided to process our samples as free floating brain section. 9 days after the MCAO procedure rats were deeply anesthetized and perfused trans-cordially with 150 ml saline followed by 300 ml 4% paraformaldehyde prepared in phosphate buffer (PB; pH=7.4). Brains were removed and postfixed in 4% paraformaldehyde for 24 h and then transferred to PB containing 20% sucrose for 2 days. Serial coronal brain sections were cut at 40 μm on a cryostat between 4.0 and -6.0 mm bregma levels. Subsequently, the samples were processed for immunohistochemistry.

Immunolabeling for Rtn4r

Every fourth free-floating brain section of MCAO-treated animals were immune-stained with antisera raised against Rtn4r (1:300, Abcam, Cambridge, MA; cat. number: ab 26291). The specificity of the labeling is suggested by single bands in western blot experiments provided by the manufacturer.

The sections were pretreated with pH6 citrate buffer at 70°C for 60 minutes, followed by 3% hydrogen peroxide for 15 min and 1% bovine serum albumin in PB containing 0.5% Triton X-100 for 30 min at room temperature. Then, the antisera (1:300) was applied for 48 h at room temperature followed by incubation of the sections in biotinylated donkey anti-rabbit secondary antibody (1:1000; Vector Laboratories, Burlingame, CA) and then in avidin-biotin-peroxidase complex (1:500; Vector Laboratories) for 1 h. Subsequently, the labeling was visualized by incubation in 0.02% 3,3-diaminobenzidine (DAB; Sigma-Aldrich, St. Louis, MI), 0.08% nickel (II) sulfate and 0.001% hydrogen peroxide in PB, for 5 min. Sections were mounted, dehydrated and coverslipped with Cytoseal 60 (Stephens Scientific, Riverdale, CA).

Double immunolabeling of Rtn4r with cell markers

The following antisera were used as cellular markers in double labeling experiments: mouse anti-NeuN as a marker of neuronal nuclei (1:500; Millipore, Billerica, MA, cat. number: MAB377), mouse anti-S-100, as a marker of astrocytes (1:5000 Sigma-Aldrich, St. Louis, MI cat. number: S2532), rabbit anti-ionized calcium-binding adapter molecule 1 (Iba1) as a marker of microglial cells (1:1000; Wako, Japan; cat. number: 019-197419), and rabbit anti-Von Willebrand factor (vWF) as an endothelial marker (1:1500 Abcam,Cambridge, MI; cat. number: ab6994).

First, free-floating sections of the 6 rats used for single labeling Rtn4r were immune-labeled for this protein, as described above, except that donkey anti-mouse secondary antibodies, cross-absorbed with IgG of several different species (including rabbit) were used to avoid cross-reactions (1:1000 dilution; Jackson ImmunoResearch, West Grove, CA). Another difference was that the labeling was visualized using fluorescein isothiocyanate-tyramide (1:8000) and H_2O_2 in Tris hydrochloride buffer (0.1 M, pH=8.0) for 6 min instead of DAB. Then, the sections intended for double labeling with Iba1 and vWF were incubated in citric

acid buffer (pH=6.0) for 30 min to remove rabbit antibodies from the sections in order to avoid cross reactions. Subsequently, all sections were placed in antibodies of the above described cell markers for 48 h at room temperature. The sections were then incubated in Alexa594 donkey anti-mouse (or anti-rabbit for Iba1) secondary antibody (1:500; Molecular Probes, Eugene, OR) for 2 h, washed in PB overnight, mounted and cover slipped in anti-fade medium (Prolong Antifade Kit, Molecular Probes, Eugene, OR).

Immunolabeling of Notch 1 intracellular domain (NICD), and Jagged 1 and RECA

Every fourth free-floating brain section of MCAO-treated animals were immune-stained with antisera raised against NICD (ABCAM, Cambridge; cat. number: ab52301), Jagged 1 (LifeSpan BioSciences, Seattle, WA, USA; cat. number: LS-C18929) and RECA (ABCAM, Cambridge, MA, USA; cat. number: ab9774). The specificity of the labeling is suggested by single bands in western blot experiments provided by the manufacturer.

The sections were pretreated with 3% hydrogen peroxide for 15 min followed by 1% bovine serum albumin in PB containing 0.5% Triton X-100 for 30 min at room temperature. Then, the antisera (1:1000 for RECA, 1:500 for NICD, and 1:100 for Jagged 1) were applied for 48 h at room temperature followed by incubation of the sections in biotinylated donkey anti-rabbit (or anti-mouse for RECA) secondary antibody (1:1000; Vector Laboratories, Burlingame, CA) and then in avidin-biotin-peroxidase complex (1:500; Vector Laboratories) for 1 h. Subsequently, the labeling was visualized by incubation in 0.02% 3,3-diaminobenzidine (DAB; Sigma), 0.08% nickel (II) sulfate and 0.001% hydrogen peroxide in PB, for 5 min. Sections were mounted, dehydrated and coverslipped with Cytoseal 60 (Stephens Scientific, Riverdale, NJ).

Double immunolabeling of NICD and Jagged 1 with cell markers

The following antisera were used as cellular markers in double labeling experiments: mouse anti-synaptophysin as a marker of neuronal presynaptic terminals (1:1000; DAKO, Ely, UK; cat. number SY38), mouse anti-glial fibrillary acidic protein (GFAP) as a marker of astrocytes (1:300; Santa Cruz Biotechnology, Delaware, CA, USA; cat. number: sc-33673), rabbit anti-ionized calcium-binding adapter molecule 1 (Iba1) as a marker of microglial cells (1:1000; Wako, Japan; cat. number: 019-197419) and mouse anti-RECA for endothelium (1:1000, ABCAM, Cambridge, MA, USA; cat. number: ab9774).

First, free-floating sections of the 12 rats used for single labeling NICD and Jagged 1 were immunolabeled for these proteins, as described above, except that donkey anti-mouse secondary antibodies, cross-absorbed with IgG of several different species (including rabbit) were used to avoid cross-reactions (1:1000 dilution; Jackson ImmunoResearch, West Grove, PA). Another difference was that the labeling was visualized using fluorescein isothiocyanate-tyramide (1:8000) and H_2O_2 in Tris hydrochloride buffer (0.1 M, pH=8.0) for 6 min instead of DAB. Then, the sections intended for double labeling with Iba1 were incubated in citric acid buffer (pH=6.0) for 30 min to remove rabbit antibodies from the sections in order to avoid cross reactions. Subsequently, all sections were placed in antibodies of the above described cell markers for 48 h at room temperature. The sections were then incubated in Alexa594 donkey anti-mouse (or anti-rabbit for Iba1) secondary antibody (1:500; Molecular Probes, Eugene, OR) for 2 h, washed in PB overnight, mounted and cover slipped in anti-fade medium (Prolong Antifade Kit, Molecular Probes).

Microscopy, photography and image processing and quantification

Sections were examined using an Olympus BX60 light microscope. Coronal sections obtained near bregma level were involved in the analysis from each animal (6 brains per group). After identification of the infarcted region 5 adjacent fields near the lesion were captured in the striatum at 2048 X 2048 pixel resolution with a SPOT Xplorer digital CCD camera (Diagnostic Instruments, Sterling Heights, MI) using 40 X objectives. The digitized images were then contrast enhanced (equally), and a thresholding procedure was used to determine the proportion of immune-reactive area within the peri-ischemic region with Image J software (NIH, Bethesda, USA). The data are presented as a percentage of positive immunoreactivity area within the captured images.

Confocal images were acquired with a Nikon Eclipse E800 confocal microscope equipped with a BioRad Radiance 2100 Laser Scanning System using a 60 X objective at an optical thickness of 2 μm. A section containing lesion at the level of the anterior commissure was randomly selected from the double labeled brains for each marker. The total number of NICD-, Jagged 1- and Rtn4r-ir cells with an identifiable cell nucleus as well as the number of double labeled cells was counted.

Western blot for Rtn4r

In order to improve the quantification of the protein end-product Western blot analysis was performed on basis of the significant mRNA expression change of the Rtn4r gene. We used NuPAGE 4-12% bistris gels (Invitrogen, Gent, Belgium), proteins were transferred to polyvinylidene-fluoride membranes, which were blocked by Tris-buffered saline/0.1% Tween-20 containing 5% dried milk powder followed by incubation in the same buffer containing the appropriate primary antibody (1:500, Anti-Rtn4 Receptor, cat. number: AF 12080, and Anti-GAPDH, cat. Number: AF 5718, R&D, Minneapolis, MI). Membranes were washed in TBST and incubated with the appropriate peroxidase-conjugated secondary antibody. Reactions were developed using HRP, and quantification was performed using the Image lab 4.0.1. software (Bio-Rad Laboratories, Hercules, CA), results were analyzed after normalization with the GAPDH control.

Statistical analysis

Normalized c-DNA expression values, and normalized protein levels were used for analysis. We used Student T test for screening calculations, and Mann-Whitney-Wilcoxon (MWW) test for confirming our result in the Graphpad Prism 6 software (Graphpad Software, La Jolla, CA).

We have not used power analysis in the planning of our experiments. While nobody contests the usefulness of power analysis in general, many more questions have been raised in the accuracy of these calculations in the setting of exploratory gene expression studies. The used algorithms can become very complex in this context, taking the multiple interactions among genes into account. While literature data clearly show that stable array results are typically not obtained until at least five biological replicates have been used, sample sizes of 5/ group usually provide sufficient power, especially in well standardized protocols using inbreed laboratory animals (Pavlidis et al., 2003). Our most important goal was to maximize the homogeneity of the experiments when we decided to limit the number of animals to 6 in each treatment group. This sample size allowed us to carry out all experiments on the same day to maximally reduce the baseline variance of gene expression occurring over time among the individual subjects.

RESULTS

Changes of mRNA expression in the peri-infarct cortex following delayed gelatinase inhibition

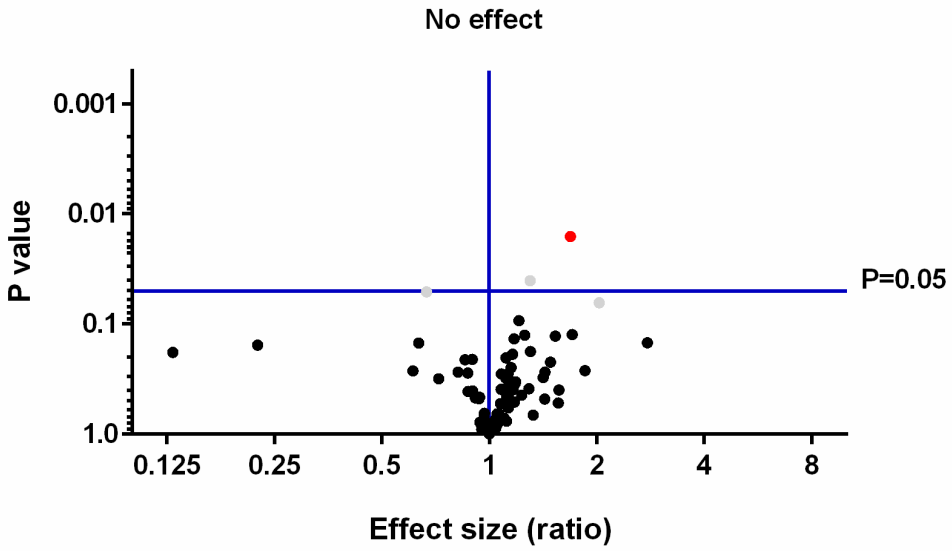

Gene	Fold change	P value	Gene	Fold change	P value	Gene	Fold change	P value	Gene	Fold change	P value
GAP43	1,13	0,46	Cspg4	0,91	0,47	Birc3	0,86	0,19	Bcl3	0,85	0,51
Jun	1,30	0,04	Nrp1	1,05	0,82	Naip2	1,64	0,26	Card10	1,03	0,71
SPRR1a	1,16	0,39	Rtn4	1,13	0,43	Bcl2l2	0,94	0,65	Cradd	0,90	0,31
Neurod6	1,04	0,88	**Rtn4r**	**1,69**	**0,02**	Bcl2l1	0,90	0,45	Sod1	1,17	0,21
Tuba1a	1,17	0,14	Ngfr	2,03	0,06	Ripk1	0,98	0,86	Sod2	0,95	0,70
L1cam	0,99	0,95	Mag	0,82	0,27	Bax	1,02	0,78	Stat3	0,96	0,75
Marcks	1,03	0,76	Mog	1,25	0,13	Bid	1,15	0,41	Csnk2b	0,93	0,28
Cuzd1	1,56	0,52	Lilrb3	0,22	0,16	Casp1	0,93	0,75	Cybb	0,54	0,26
Nefm	1,18	0,33	Notch1	1,11	0,20	Casp2	1,00	0,98	Gpx1	0,97	0,88
DCC	0,67	0.05	Jag1	1,14	0,34	Casp3	1,00	0,98	Cat	0,89	0,28
Igf1	1,43	0,48	Tnf	0,70	0,27	Casp6	0,85	0,35	Hif1a	0,93	0,39
Igfbp6	0,95	0,90	Icam1	0,77	0,18	Casp7	0,83	0,09	Mmmp9	0,67	0,22
Cxcl12	1,56	0,40	Vcam1	1,07	0,48	Casp8	0,87	0,25	Plat	1,07	0,46
Vegfa	1,07	0,52	Sele	0,65	0,13	Casp9	1,03	0,64	Timp1	0,81	0,44
Kdr	0,94	0,78	Tgfb1	0,91	0,71	Casp12	0,71	0,31	Timp2	0,96	0,74
Flt1	1,05	0,65	Infg	0,75	0,67	BCL2l11	0,78	0,38	Timp3	1,00	0,99
Ngf	1,13	0,58	Hspa1a	1,58	0,15	Fadd	0,92	0,39	Timp4	1,11	0,40
Bdnf	1,12	0,76	Procr	1,39	0,31	Apaf1	1,15	0,28	Mmp2	0,59	0,12
Ncan	1,02	0,90	F2r	1,00	0,99	Diablo	1,12	0,21	Mmp12	0,36	0,15
Ptprz1	1,12	0,42	Xiap	0.89	0,32	Cycs	1,03	0,78			

Figure 14. Graphic (A) and numerical display of mRNA expression changes induced by gelatinase inhibition in the delayed phase of focal ischemia. The p values are calculated by T-test. Result show the classical volcano plot distribution with obvious induction of one gene (Rtn4 r /red dot) and borderline expressional changes of 3 others (Dcc, C-Jun, Ngf/gray dots) (Nardai et al., 2016).

Prior to the mRNA analysis, the in situ zymography of our samples demonstrated a mean 81% decrease of the gelatinase activity in the peri-infarct cortical regions of the treatment animals compared to the controls (p=0,008) following the intra-cerebroventricular injection of the FN-439 inhibitor (Fig. 15), similarly to previously published data.

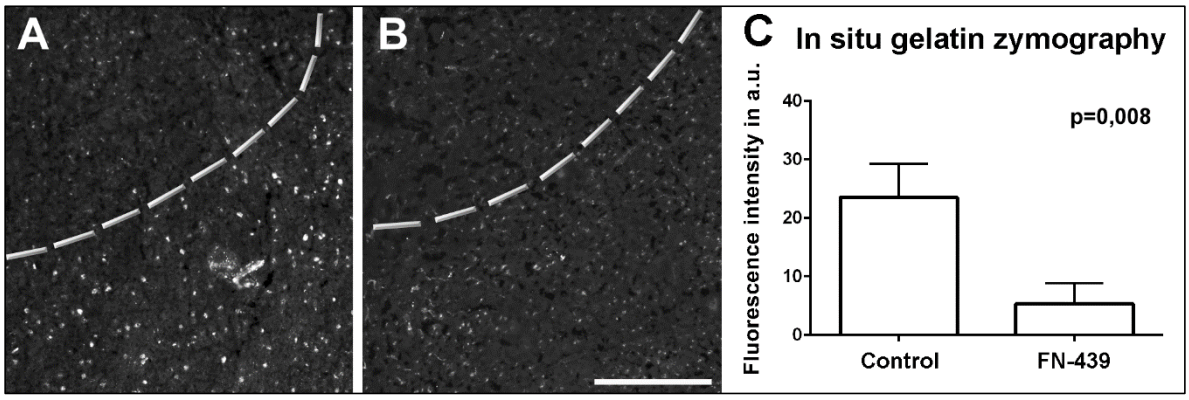

Figure 15. Gelatinase activity in the peri-infarct cortex. Gray lines indicate the border of the lesion. The distribution of the fluorescence signal following the gelatinase inhibition (B) is similar to the non-treated controls (A), but the number and size of the spot is clearly decreased. The columns on the right (C) show the quantification of the immunofluorescence signal intensity. Error bars represent SEM (Nardai et al., 2016).

The successfully tested 84 genes involved in synaptic plasticity, apoptosis regulation, reperfusion injury, and neurovascular remodeling (Fig. 14) could be regrouped into three categories based on their response to the delayed (day 7) gelatinase inhibition. The vast majority of the tested mRNAs (n=80) showed unaltered expression, while the Reticulon 4 receptor (Rtn4r) was clearly induced in the cortex of the treated animals (Fold change: 1,69, p=0,015 by T-test, p=0,028 by MWW test) (Fig. 16.). We found altered expression with borderline statistical significance in three additional genes: the expression of the C-jun protooncogene (Jun)showed a 30% increase (p=0.040 by the T-test, p=0.075 by MWW),the Nerve growth factor receptor (Ngfr) showed a mean 2,03 fold increase (p=0.064 on the T-test, p=0.032 by MWW), while the mRNA level of the Deleted in colorectal carcinoma (DCC) axonal guidance receptor was decreased by 33% (p=0.051 on the T-test, p=0.008 by MWW) compared to the untreated controls (Fig. 14).

Rtn4r protein expression following MCAO and its alteration by gelatinase inhibition

Rtn4r immunoreactivity under normal conditions is unevenly distributed in the intact brain tissue both in the striatum and the cerebral cortex [15]. Following MCAO, Rtn4r appears in the peri-infarct region around the lesion without any labeling within the lesion (Fig. 16A). In fact, the border of the lesion can be defined clearly based on the Rtn4r histochemistry. The labeling in the peri-infarct region is present in cell bodies. Following Fn439 treatment, the distribution of Rtn4r labeling did not change as compared to control MCAO (Fig. 16B), however the intensity of the immunolabeling was markedly elevated in the peri-infarct region.

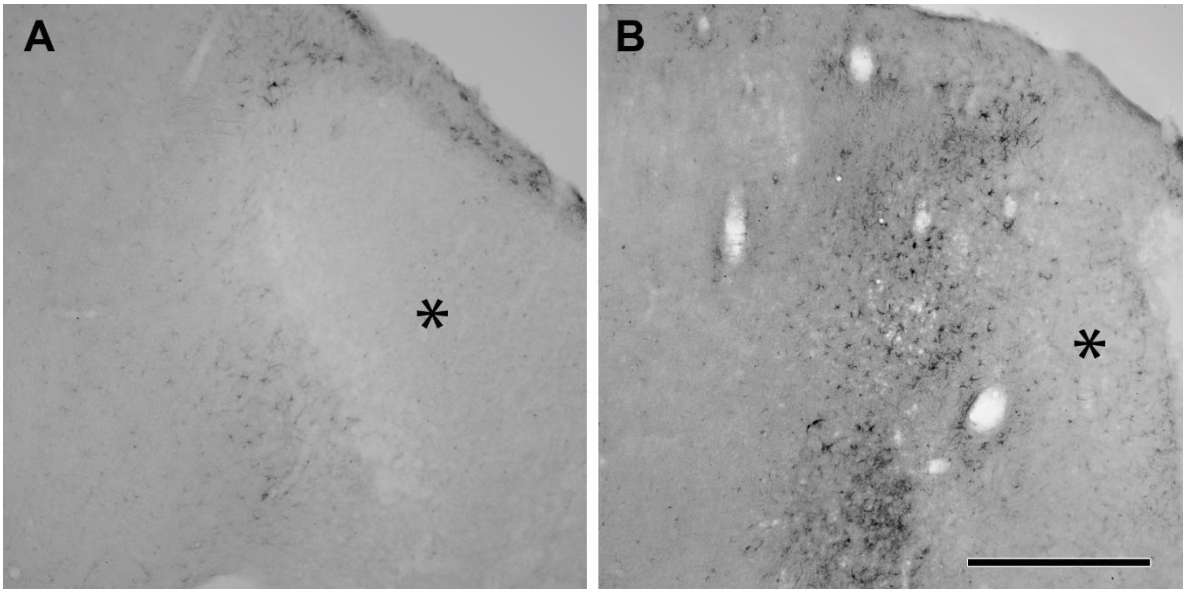

Figure 16. Rtn4r immunoreactivities in the peri-infarct region of the cerebral cortex. A: Rtn4r labeling is elevated in the peri-infarct region, the appearance of labeling indicates the border of the lesion. B: The distribution of Rtn4r following gelatinase inhibitor treatment is similar to that of non-treated MCAO but an increased intensity of Rtn4r labeling is in response to the FN439 treatment. Star symbols (*) indicate the lesioned areas. Scale bar = 500 μm (Nardai et al., 2016).

Confirmation of the increased Rtn4r protein abundancy by Western Blot

In order to better quantify the Rtn4r protein expression in the peri-infarct cortex, we have performed western blotting analysis of the native brain samples. The blots have also confirmed the increased protein level for the Rtn4 receptor (p= 0,004) in the treated animals (Fig 17B).

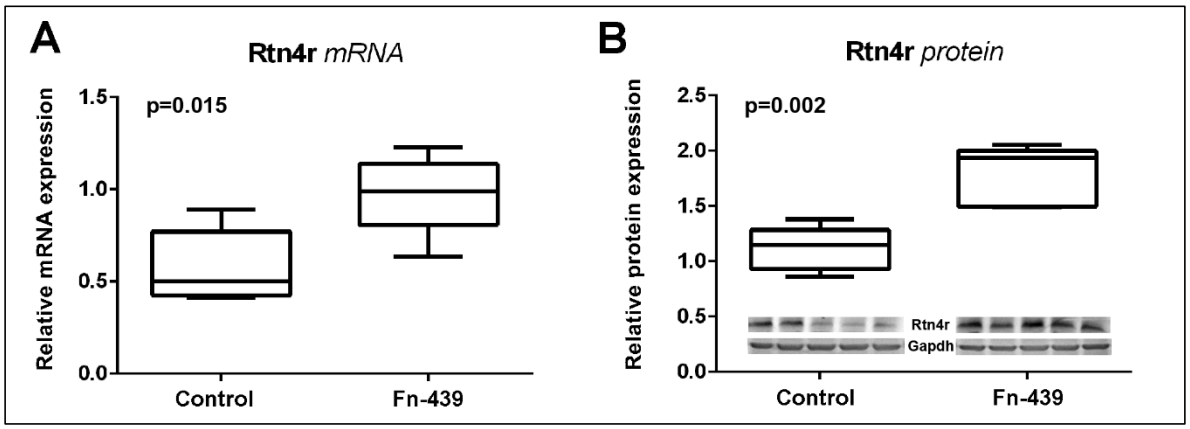

Figure 17. Box and whiskers show the relative mRNA (A) and protein (B) expression level of the Rtn4r in the peri-infarct cortex following delayed (day 7) gelatinase inhibitor treatment. P-values were calculated by T-test. Insert show the original blot image. Error bars represent minimal to maximal values (Nardai et al., 2016).

Double immunolabeling of Rtn4r with cell markers

S100 immunohistochemistry labeled astrocytes with the characteristic processes. We found that essentially all Rtn4r labeled cells were double labeled with S100 (98,1%) suggesting their expression in astrocytes (Fig. 18C). The Rtn4r immunoreactivity was present in the cell bodies and the foot processes of the astrocytes. In contrast, microglial cells labeled by the marker Iba1 do not contain Rtn4r (Fig. 18d). Neuronal cell bodies in the peri-infarct cortex did not co-localize with the Rtn4r either, however we noted altogether a weaker NeuN staining in this region, which may also contribute to the lack of double labeling (Fig. 18a). Finally the double staining with the vWF endothelial marker did not overlap with the Rtn4r arguing against the expression of the latter in the vasculature.

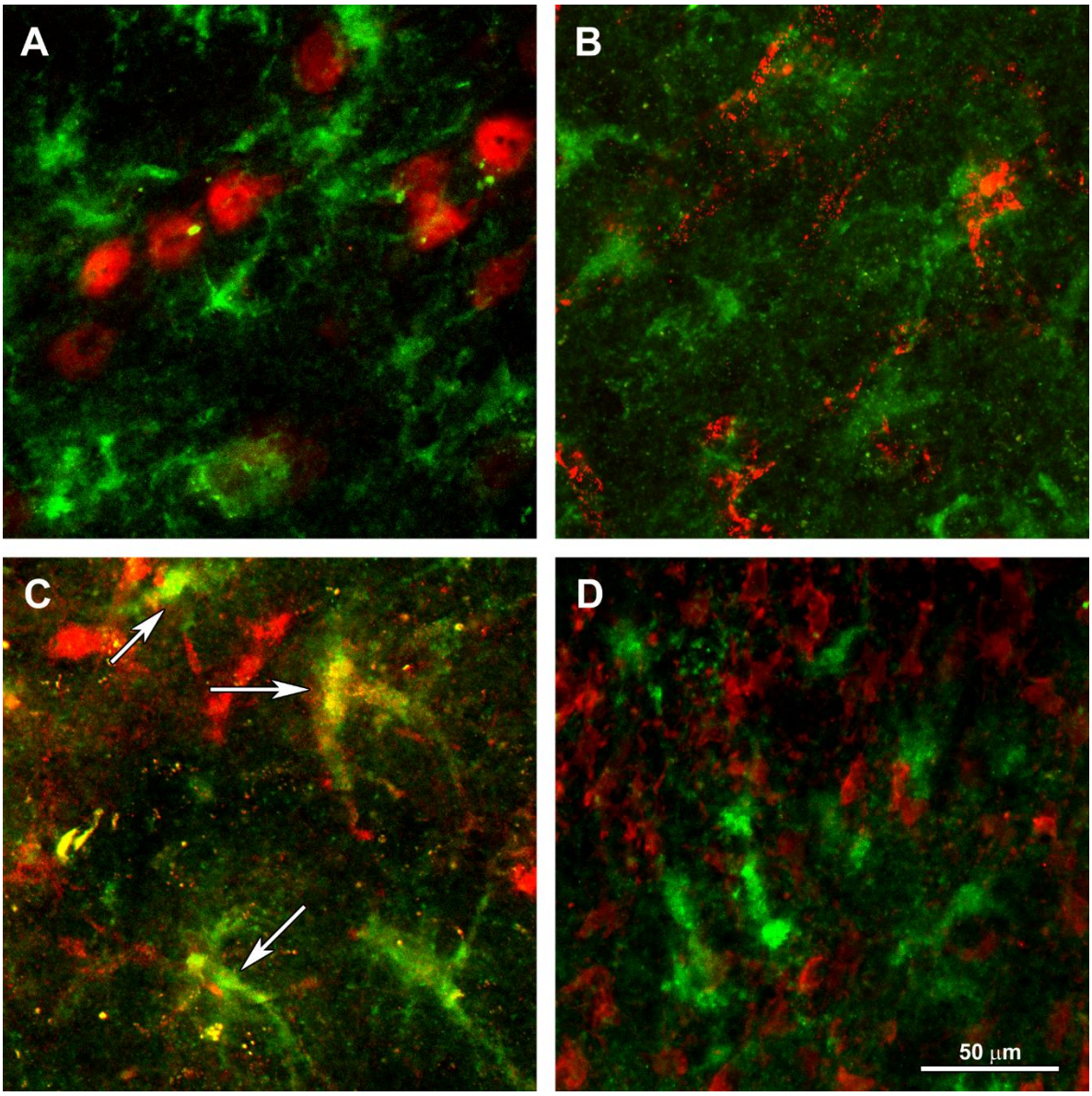

Figure 18. Demonstration of the presence of Rtn4r 1 in astrocytes but not in other cell types. In all panels, Rtn4r is green and the other markers are labeled red. Clear co-localization is shown with the S100 astrocyte marker (arrows) (C) while double labeling with NeuN (A) with vWF (B) and Iba1 (D) show no co-localization with the Rtn4r indicated by the lack of yellow labeling. Scale bar = 50 μm (Nardai et al., 2016).

Selegiline induces Notch-Jagged signaling, anti-apoptosis markers, and the expression of glia associated genes

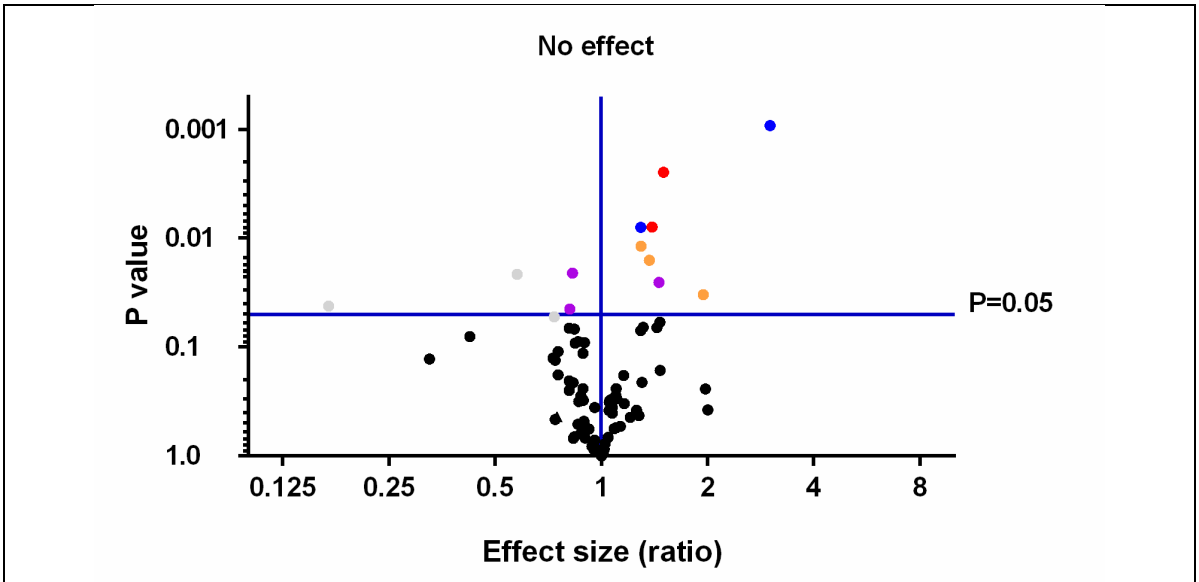

Gene	Fold change	P value	Gene	Fold change	P value	Gene	Fold change	P value	Gene	Fold change	P value
GAP43	1.47	0.16	Nrp1	0.94	0.81	Birc3	1.43	0.07	Bcl3	1.10	0.56
Jun	1.04	0.67	Rtn4	0.85	0.09	Naip2	1.25	0.38	Card10	0.89	0.02
SPRR1a	0.74	0.43	Rtn4r	1.16	0.32	Bcl2l2	0.95	0.71	Cradd	0.88	0.24
Neurod6	0.96	0.86	Ngfr	0.87	0.62	Bcl2l1	3.00	0.00	Sod1	0.96	0.36
Tuba1a	1.05	0.31	Mag	1.36	0.02	Ripk1	0.83	0.07	Sod2	0.88	0.28
L1cam	0.89	0.49	Mog	1.29	0.01	Bax	0.07	0.36	Stat3	1.10	0.30
Marcks	1.00	1.00	Lilrb3	2.00	0.38	Bid	0.83	0.21	Csnk2b	1.08	0.29
Cuzd1	1.97	0.24	Notch1	1.39	0.01	Casp1	0.81	0.20	Cybb	0.83	0.69
Nefm	0.95	0.81	Jag1	1.50	0.00	Casp2	1.10	0.24	Gpx1	0.73	0.13
DCC	1.21	0.44	Tnf	0.42	0.08	Casp3	0.89	0.31	Cat	0.90	0.09
Igf1	1.13	0.53	Icam1	0.73	0.06	Casp6	0.91	0.07	Hif1a	1.05	0.32
Igfbp6	0.73	0.13	Vcam1	1.29	0.07	Casp7	1.01	0.92	Mmmp9	0.75	0.18
Cxcl12	1.28	0.42	Sele	0.89	0.68	Casp8	1.05	0.38	Plat	1.47	0.06
Vegfa	0.92	0.56	Tgfb1	0.75	0.10	Casp9	1.01	0.85	Timp1	1.10	0.54
Kdr	0.86	0.31	Infg	0.75	0.46	Casp12	1.30	0.21	Timp2	0.89	0.11
Flt1	1.10	0.40	Hspa1a	0.95	0.86	BCL2l11	0.89	0.48	Timp3	0.84	0.09
Ngf	0.89	0.54	Procr	0.57	0.02	Fadd	1.02	0.77	Timp4	0.81	0.24
Bdnf	0.83	0.66	F2r	1.31	0.07	Apaf1	0.81	0.04	Mmp2	0.86	0.51
Ncan	1.15	0.18	Xiap	1.29	0.01	Diablo	1.45	0.03	Mmp12	0.33	0.13
Ptprz1	1.94	0.03	Proc	0.17	0.04	Cycs	1.10	0.28			

Figure 19. Graphic (A) and numerical display of mRNA expression changes induced by selegiline treatment following focal ischemia. The p values are calculated by T-test. Colors indicated the 4 groups of genes with altered expression: Notch-Jagged signaling (red: Noth1, Jag1), glia associated genes (orange: Ptprz1, Mag, Mog), anti-apoptotic (blue:Bcl2/1, Xiap) and pro-apoptotic (purple: Apaf 1, Diablo, Card10) genes. Gene expressional changes not confirmed by MWW test are shown in gray (Proc, Procr, Icam).

We successfully tested 80 representative genes involved in synaptic plasticity, apoptosis, reperfusion injury and the regulation of neurovascular remodeling following selegiline treatment in focal ischemia (Fig. 19). We evaluated the results using student T-test for the screening calculation and MWW test for confirmatory analysis. Only the expressional changes found to be significant by both test were regarded relevant. We found a significant change in the expression of 4 group of genes in the selegiline treated animals compared to the controls (Fig. 19).

Genes with anti-apoptotic properties were selected for the test because of the previously established anti-apoptotic property of selegiline. Indeed, we found significant changes in the level of 2 anti-apoptotic genes, XIAP ($p=0.01$ on T-test and $p=0.02$ by MWW) and BCL 2/1 ($p=0.00$ by both T-test and MWW). Further supporting this effect, a simultaneous down regulation of two pro-apoptotic genes Apaf1 ($p=0.04$ both on T-test and MWW) and Card 10 ($p=0.02$ by both tests) was documented. Interestingly we found Smac/Diablo, a pro-apoptotic antagonist of the XIAP to be also upregulated ($p=0.03$ by T-test, 0.04 by MWW), suggesting a potential feed-back mechanism that would need further exploration. Since the anti-apoptotic properties of selegiline have been studied before, we used the confirmation of previously established effects to validate our model but did not plan further investigations on these findings.

Genes involved in the regulation of neurovascular remodeling are very important factors influencing functional recovery. In this group we identified 2 genes, which significantly changed their expression level in the peri-infarct regions in response to selegiline treatment. The increase of the mRNA level of Notch 1 was highly significant ($p=0.01$ by both T-test and MWW), but the ligand of Notch 1, Jagged 1 also elevated its expression level ($p=0.01$ by both tests).

The forth group of genes with altered expression were the glia associated genes, who are traditionally regarded as inhibitors of plasticity. The upregulation of the myelin associated glycoprotein (Mag) ($p=0.02$ by T-test, $p=0.03$ by MWW), the oligodendrocyte glycoprotein (Mog) ($p=0.01$ by both tests) and the induction of Ptrz1 ($p=0.01$ by T-test, $p=0.02$ by MWW) already suggest that the treatment effect of selegiline involves the astrocytes.

NICD and Jagged 1 immunoreactivities following MCAO and their alterations by selegiline

NICD immunoreactivity is very low in the intact brain tissue both in the striatum and the cerebral cortex. Following MCAO, NICD appears in the peri-infarct region around the lesion without any labeling within the lesion (Fig. 20A). In fact, the border of the lesion can be defined in a straightforward way based on NICD immunohistochemistry. The labeling in the peri-infarct region is present in cell bodies and some parenchymal staining is also present. Following selegiline treatment, the distribution of NICD labeling did not change as compared to control MCAO (Fig. 20B). It was abundant at the border of the lesion but not in the intact cerebral cortex and striatum, and remained absent within the lesion. However, the intensity of NICD immunolabeling was elevated in the peri-infarct region around the lesion with a local distribution in cell bodies and parenchyma similar to that without treatment (Fig. 20B).

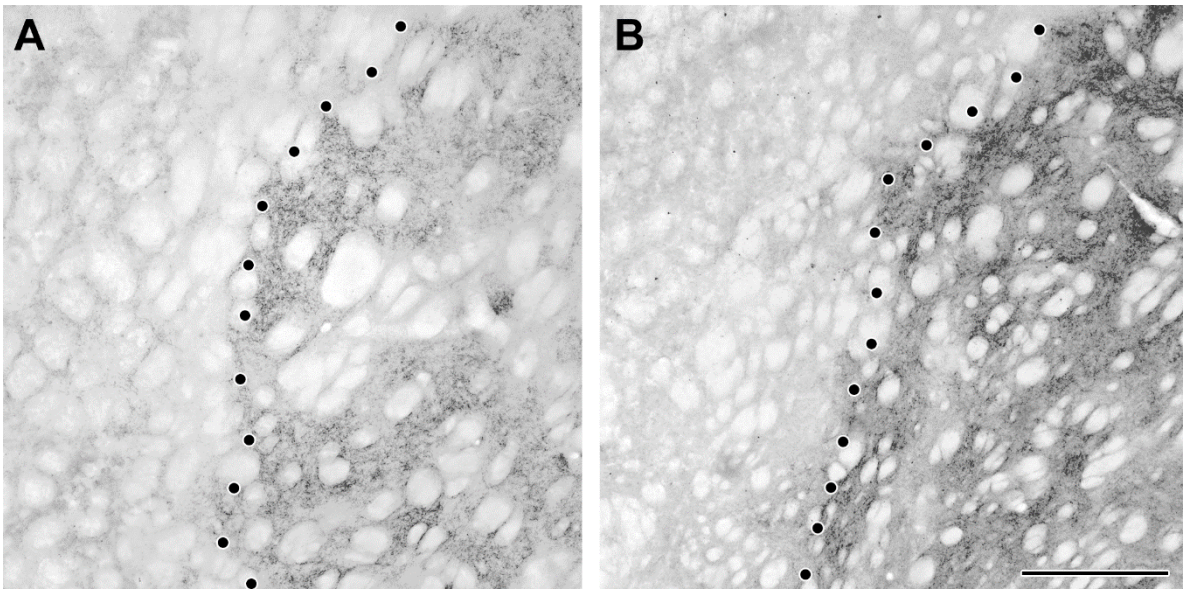

Figure 20. NICD immunoreactivities in the peri-infarct region of the striatum. A: NICD labeling is elevated in the peri-infarct region. Notch immunoreactivity is present in the gray matter but not within fiber bundles. Notch labeling is absent in the infracted tissue. The appearance of labeling indicates the border of the lesion (dotted line). B: The distribution of NICD following selegiline treatment is similar to that of non-treated MCAO but an increased intensity of NICD labeling is in response to selegiline. Star symbols (*) indicate the lesioned areas. Scale bar = 400 μm (Nardai et al., 2015).

Jagged 1 immunoreactivity is present in few scattered cells in the intact tissue. MCAO increases the number of labeled cells in the peri-infarct region (Fig. 21A). However, cells are not visible any more within the lesion. Instead, a background-like labeling of the infracted tissue appears without clear topography. In rats treated with selegiline, the labeling of the infracted tissue is the same as in controls. More importantly, the number of labeled cells as well as their labeling intensity is increased in the peri-infarct region (Fig. 21B). This enhancement of Jagged 1 immunoreactivity does not occur in the intact tissue where the density of labeled cells and their labeling intensity is similar to that of non-treated animals.

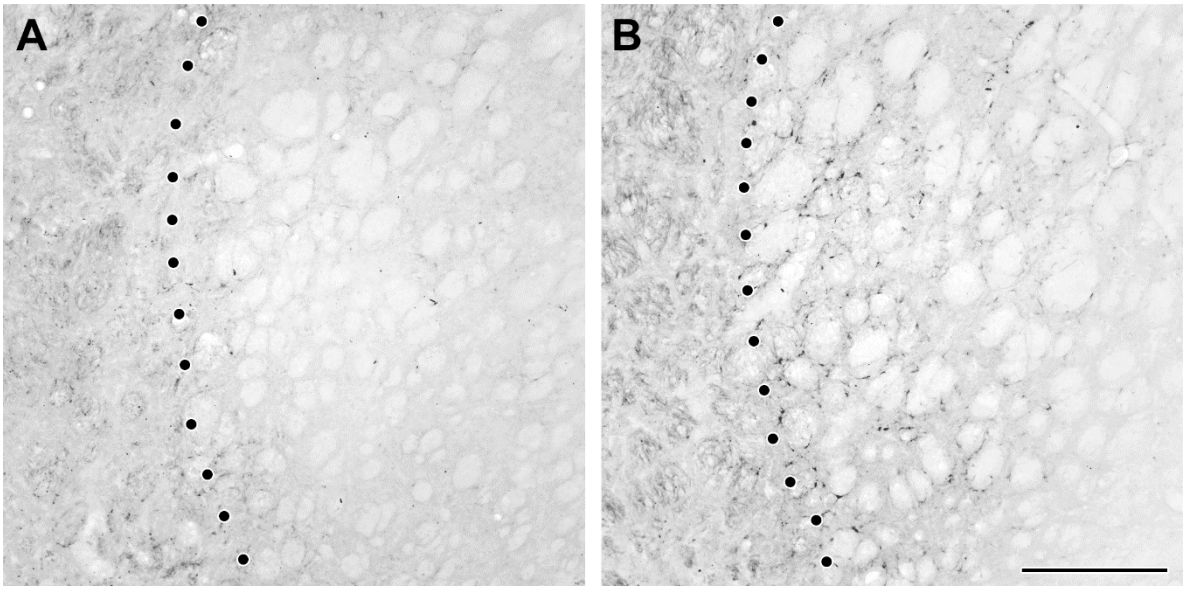

Figure 21. Jagged 1 immunoreactivity in the peri-infarct region of the striatum**.** A: There is some labeling present within the lesion without clear morphological features. Outside the lesion, some Jagged 1-immunopositive cell bodies are seen in the control MCAO rat, mostly in the gray matter around fiber bundles. B: In response to selegiline, an increased number of intensively labeled cells are present in the peri-infarct region. The background staining of the infracted tissue is similar to that of without selegiline. The lesion is indicated by star symbols (*) while the border of the lesion in shown by dotted lines. Scale bar = 400 μm (Nardai et al., 2015).

Quantitative measurement of immunolabeling indicated increased level NICD and Jagged 1 in the peri-infarct region of selegiline-treated rats as compared to control animals with MCAO lesion (Fig. 22). The ratio of immunolabeled area increased from 32.10% to 51.31% (p=0.027) for NICD, from 2.33 % to 17.68 % (p=0.031) for Jagged 1.

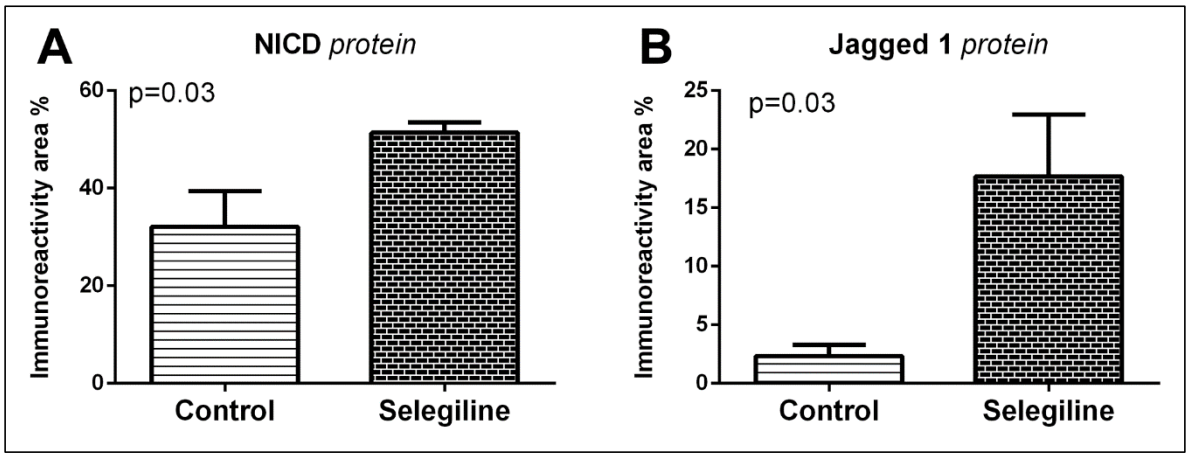

Figure 22. The effect of selegiline on the immunolabeled area % in the peri-infarct region using NICD, and Jagged 1 immunosera. Columns demonstrate significantly increased immunolabeling in the selegiline treated animals compared to controls. Bars display immunoreactivity area percentage, error bars represent SEM (Nardai et al., 2015).

Double immunolabeling of NICD and Jagged 1 with cell markers

NICD and Jagged expression have been documented on various cell types within the central nervous system before, therefore we used double labeling to better characterize the expression changes induced by selegiline.

GFAP immunohistochemistry labeled astrocytes with the characteristic processes. We found that essentially all NICD and Jagged 1 neurons were double labeled with GFAP (97.1%, and 94.9%, respectively) suggesting their expression in astrocytes (Fig.23A). Both immunoreactivities were present in cell bodies as well as in processes of astrocytes. In contrast, microglial cells labeled by the marker Iba1 and endothelium shown by RECA do not contain NICD and Jagged 1 (Fig. 23B). Neuronal cell bodies were not examined due to the disappearance of NeuN in the penumbra, however, the presynaptic marker synaptophysin did not co-localize with either NICD or Jagged 1 arguing against their presence in presynaptic terminals (Fig. 23C).

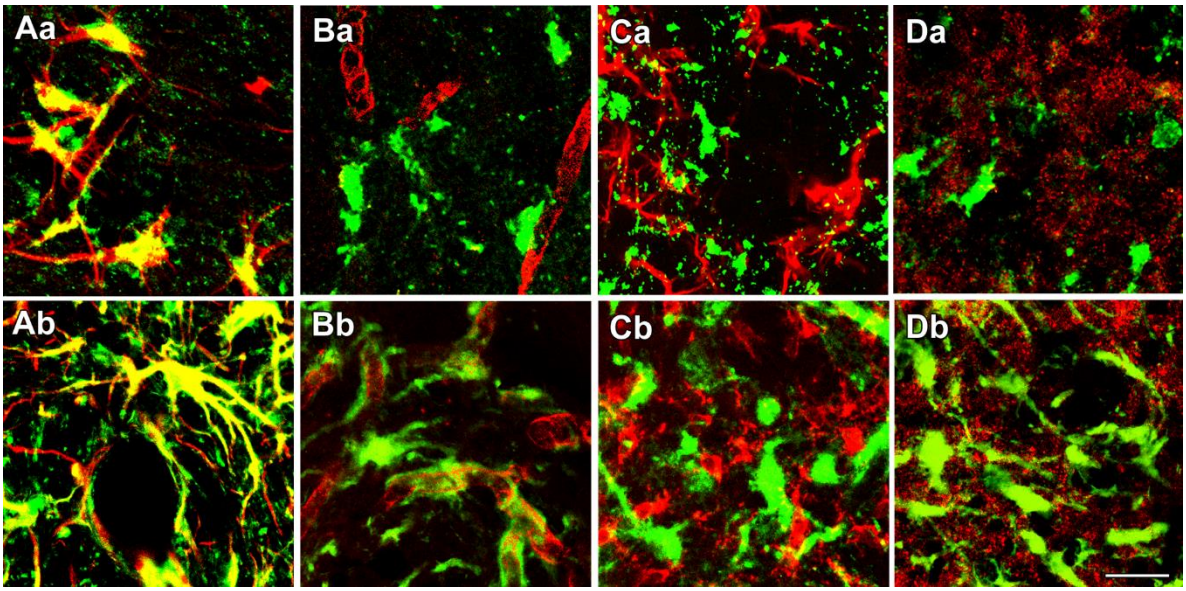

Figure 23. Demonstration of the presence of NICD and Jagged 1 in astrocytes but not in other cell types. In all panels, NICD or Jagged 1 are green and the markers are labeled red. A: Double labeling with GFAP. Both NICD (Aa) and Jagged 1 (Ab) co-localize with GFAP (yellow). B: Double labeling with RECA do not show NICD and Jagged1 in close proximity of the vascular structures, but no co-localization. C: Double labeling with Iba1. Neither NICD (Ba) nor Jagged 1 (Bb) co-localize with Iba1 indicated by the lack of yellow labeling. D: Neither NICD (Ca) nor Jagged 1 (Cb) co-localize with synaptophysin indicated by the lack of yellow labeling. Scale bar = 20 μm (Nardai et al., 2015).

Measurement of microvascular density by RECA immunolabeling

Microvascular density has a profound impact on cerebral edema resorption, therefore we decided the measure the effect of selegiline treatment on the peri-infarct capillaries. Blood vessels labeled by RECA largely disappear within the lesion. Their density is markedly reduced in the infracted tissue (Fig. 24A). In contrast, the peri-infarct region possesses an elevated density of capillary network as compared to that in the intact tissue. The difference between the lesion and its surroundings is so outstanding that the border of the lesion can be delineated based on RECA staining (Fig. 24A). Selegiline has a pronounced effect on the density of capillaries. In selegiline-treated animals, the density of the capillary network is somewhat higher in parts of the lesion that are in the vicinity of its borders (Fig. 24B).

Furthermore, the number of capillaries is increased in the peri-infarct region of selegiline-treated animals as compared to the same area of control animals (Fig. 24B).

Quantitative measurement of immunolabeling indicated increased level of RECA in the peri-infarct region of selegiline-treated rats as compared to control animals with MCAO lesion (Fig. 24, Fig. 26B). The ratio of immune-labeled area increased from 23.00% to 31.15% (p=0.037).

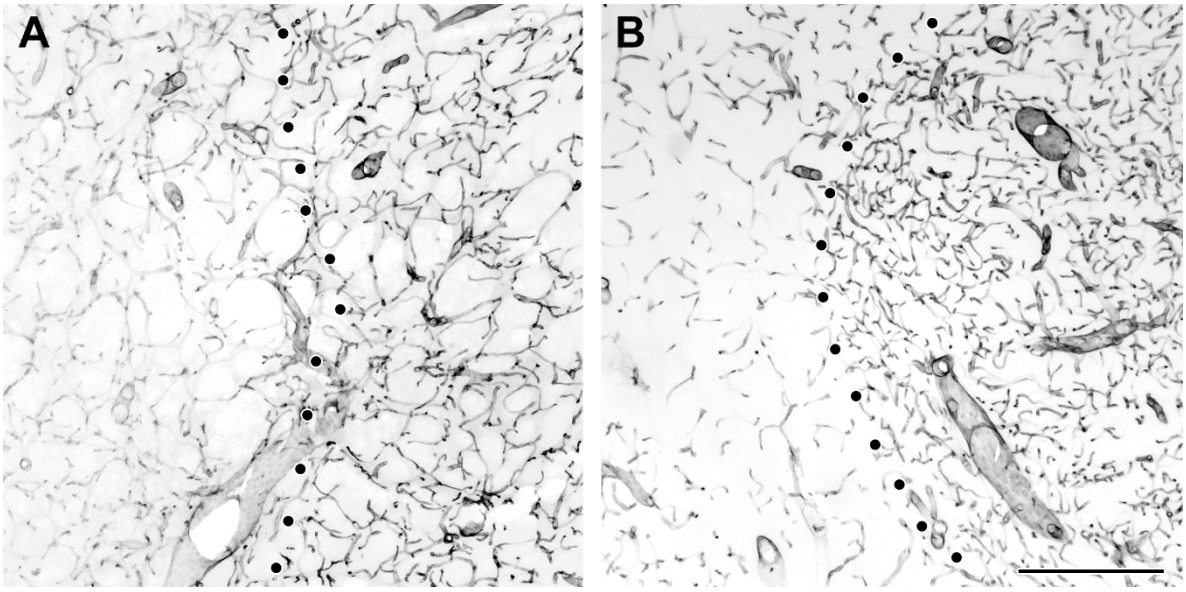

Figure 24. RECA immunoreactivities at the border of the lesion in the striatum. A: RECA labels endothelial cells of blood vessels within the lesion as well as outside of it. Most of the vessels are small capillaries. Noticeably, the density of capillary network is low within and high outside the lesion. B: Selegiline treatment increases the density of capillaries the border of the lesion both within and outside the border of the lesion. The lesion is indicated by star symbols (*) while the border of the lesion in shown by dotted lines. Scale bar = 400 μm (Nardai et al., 2015).

MRI measurement of edema

tMCAO treatment resulted in a significant edema, whose extent was possible to be visualized by whole brain MRI of the experimental animals 8 days after tMCAO (Fig. 25A). We found significantly decreased edema by selegiline treatment compared to controls (Fig. 25B; Fig. 26A; p=0.047).

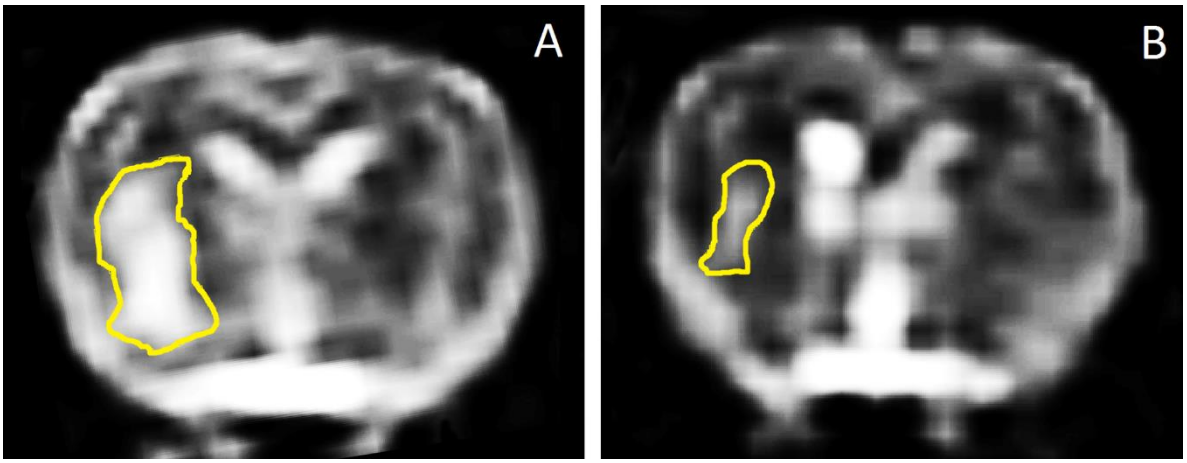

Figure 25. Peri-lesional edema visualized by T2 weighted 3D VISTA sequence on a 1,5 Tesla MRI system using SENSE-Flex-M coil 8 days after 60min tMCAO on selegiline treatment (B) compared to control (A). Despite suboptimal image quality due to the use of human clinical scanner, the image resolution was sufficient for standardized edema measurements. Indeed, the white areas indicated by the yellow lines in the left hemispheres of the representative images demonstrate a reduced edema following selegiline treatment (Nardai et al., 2015).

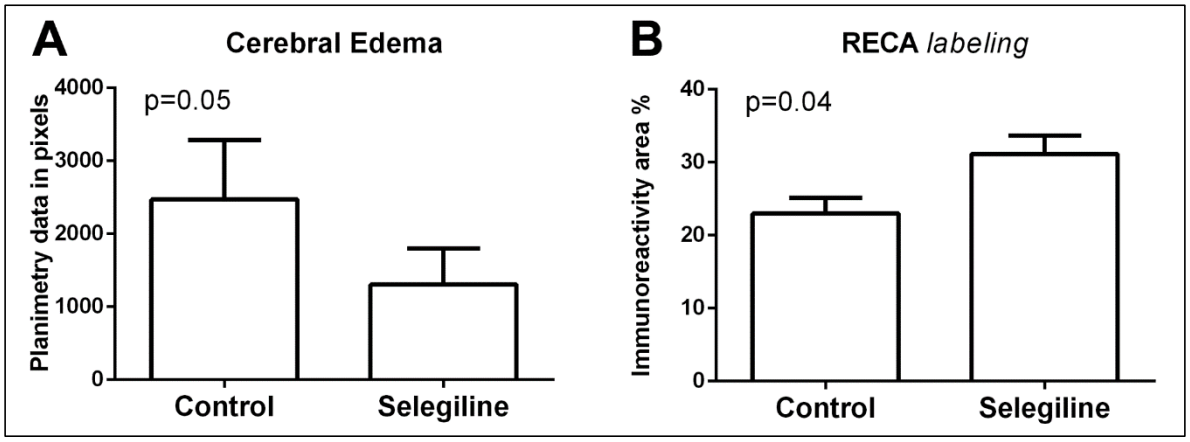

Figure 26. The effect of selegiline treatment on cerebral edema and microvascular density. Columns demonstrate significantly decreased planimetric area of cerebral edema in the selegiline treated animals (A), while the microvascular density shown by RECA immunoreactivity is increased in comparison to controls. Error bars represent SEM (Nardai et al., 2015).

DISCUSSION

The complex role of astrocytes in the neurovascular unit

Historically, glial cells were thought to constitute a barrier to repair in neuronal injuries due to their inhibition of axonal sprouting (Pekny et al., 2014). It is now widely accepted that reactive astrocytes are beneficial in preserving neuronal tissue by isolating the injury, thereby preventing further damage to the adjacent structures (Bush et al., 1999; Li et al., 2008; Ridet et al., 1997; White and Jakeman, 2008). Indeed, astrocyte proliferation is also required for neovascularization and barrier-genesis following ischemic injury (Lee et al., 2009; Quaegebeur et al., 2011). A complex interplay of concomitant processes involving the neurovascular unit influence recovery**,** and whether the proliferating astrocytes would lead to scar formation or the restoration of the physiologic barriers is highly determined by extent of the parallel microvascular rearrangement.

We tested two fundamentally different pharmacological approaches, gelatinase inhibition and selegiline treatment. While the previous studies demonstrated opposite effect of these interventions on functional recovery in the subacute phase of cerebral infarction, our experiments have shown that they both primarily induce gene expressional changes in astrocytes following large vessel occlusion.

The reason for these paradox findings lay probably in the fundamentally different effect of the two treatments on microvascular remodeling. Gelatinase inhibition in the subacute phase of focal ischemia was shown to suppress neurovascular remodeling. The exogenous administration of VEGF in a rescue experiment could prevent the MMP-induced worsening of the infarction by accelerating neovascularization (Zhao et al., 2006).

In contrast, Selegiline treatment has been previously shown to exert a cytoprotective effect on human brain capillaries in vitro (Denes et al., 2006). Using RECA immunolabeling, we also found an increased microvascular density in the peri-infarct region of the selegiline treated rats compared to controls (Fig. 24). These findings further underlie the importance of interpreting our results in accordance with to the neurovascular unit concept.

Induced Rtn4r expression in the astrocytes of the peri-infarct region following gelatinase inhibition

We have found significantly increased Rtn4r expression in the astrocytes of the peri-infarct region following gelatinase inhibition in the subacute phase of cerebral infarction. According to literature data the gelatinase enzymes show a biphasic activation pattern following focal cerebral ischemia: the acute activation in the ischemic core is primarily associated with the invading granulocytes (Opdenakker et al., 2001), and the second, sub-acute activity peak involves the NeuN+ neurons and GFAP+ astrocytes of the peri-infarct cortex (Zhao et al., 2006). While the inhibition of the leucocyte-associated acute MMP activity helped to preserve the neural tissue in previous stroke experiments, functional recovery was impaired by the pharmacological inhibition of the delayed, cortical gelatinase activity (Zhao et al., 2006). The elevated Rtn4r expression documented in our study represent a potential new mechanism contributing to this deleterious effect.

The Rtn4r is a principal member of the NOGO system: the myelin components inhibit neurite outgrowth by binding to the neuronal Rtn4 receptor, that transduces the inhibitory signal to the cell interior via its co-receptor, Ngfr (GrandPre et al., 2002). Previously published data confirmed, that the metalloproteinase mediated shedding of the Rtn4r results in the release of a soluble N-terminal fragment of the receptor, which adheres to the Ngfr-Rtn4r complex and blocks its signal transmission (Walmsley et al., 2004).

While the NOGO mediated axonal regrowth-inhibition after stroke has been primarily attributed to the neuronal Rtn4 receptors, the same protein was shown to promote the astroglial differentiation of the neural progenitor cells in vitro (Wang et al., 2008). Our results suggest, that the higher abundancy of Rtn4r positive astrocytes found in the peri-infarct cortex of the treated animals following delayed gelatinase inhibition may be a consequence of the increased astroglial differentiation of the neural progenitors, as a result of the augmented NOGO signaling, due to the lack of the Rtn4 receptor shedding.

In the peri-infarct cortex we have found an almost exclusive co-localization of the Rtn4r with the S100 astrocyte marker. No neuronal co-labeling was documented, despite the literature data supporting the expression of the receptor on neurons in the normal rat brain (Funahashi

et al., 2008). Important to note however, that the standardly used NeuN neuronal marker has a tendency to lose immunogenicity in the peri-infarct region (Unal-Cevik et al., 2004), therefore the lack double labeling in our experiments does not exclude the potential expression of the Rtn4r on neurons.

While the new data on the upregulation of the Rtn4 receptor expression in the peri-infarct cortex helps to explain the impaired regeneration associated with delayed MMP inhibition in ischemic stroke, many questions are still unanswered. The exact mechanism by which the gelatinase inhibitors enhance the mRNA expression of the Rtn4r remains to be explored, and future experiments are needed to clarify how the potentially increased NOGO signaling associated with the delayed gelatinase inhibition may affect the neurons in the peri-infarct region.

Important to note, that the potentially increased astroglial differentiation of the neural progenitors in the peri-infarct cortex was detected following delayed gelatinase inhibition, a treatment known to suppress neurovascular remodeling. Without the parallel reconstitution of the microvascular bed, the proliferation of astrocytes would rather lead to glial scar formation, than to the restoration of physiologic barriers, explaining the detrimental effect of the treatment on functional outcomes.

Notch signaling following MCAO

Notch signaling plays an important role in the development of the nervous system. However, the expression of its components are diminished in the adult brain (Irvin et al., 2004; Irvin et al., 2001; Stump et al., 2002). We found that Notch 1 and Jagged 1 mRNA levels were increased in the peri-infarct region of MCAO treated rats. The elevation in mRNA levels translated to an increase in protein levels based on the immune-histochemical analyses. These results confirmed previous data for Notch 1, which has been shown to be induced by global ischemia (Oya et al., 2009) as well as in the peri-infarct region of MCAO lesions (Zhang et al., 2012). Furthermore, our result that Notch 1 is expressed in astrocytes in the peri-infarct region following MCAO is also in agreement with previous findings (Shimada et al., 2011). In contrast, Jagged 1, a ligand of Notch 1, has not been previously reported following MCAO. Thus, our result that Jagged 1 is also induced by MCAO in the same region where Notch 1

appears is novel and further suggests the activation of Notch-Jagged signaling in response to ischemia. Because the Notch signaling system is known to be involved in a variety of developmental and morphological alterations of cells, it may play a similar role in astrocytes following injury. Indeed, the actual function of Notch 1 induced in astrocytes has recently been addressed. A γ-secretase inhibitor of Notch signaling, as well as selective inhibition of Notch 1 signaling in astrocytes, reduced reactive astrocyte formation in the peri-infarct area 3 days after MCAO, suggesting that Notch 1 signal transduction plays a critical role in reactive gliosis (Shimada et al., 2011). As both the ligand and the receptor are induced in astrocytes following an ischemic challenge, the Notch-Jagged signaling system is ideally positioned to play a part in astrocyte-astrocyte communication following neuronal injury.

The influence of Notch signaling on the outcome of stroke is highly dependent on the site of activation and the cell types involved. Although Notch 1 activation in neurons and inflammatory cells may worsen the outcome (Arumugam et al., 2011; Wei et al., 2011), Notch 1 signaling in neural stem cells and progenitor cells promotes recovery (Wang et al., 2009). Notch 1 activation in proliferating reactive astrocytes is also thought to play a beneficial role as it was shown to protect the brain following focal ischemia possibly by decreasing immune cell invasion into the injured territories (Shimada et al., 2011). Notch 1 may also promote regeneration by inducing angiogenesis. In was shown that Notch 1 induces a pro-angiogenic state in normal vasculature (ZhuGe et al., 2009). Furthermore, the Notch signaling pathway was also shown to be involved in stroke-induced angiogenesis in the ischemic brain (Guo et al., 2012; Zacharek et al., 2009).

The effect of selegiline following focal ischemia

Selegiline increased mRNA levels of Notch 1 and its ligand Jagged 1, but no other examined genes were involved in the remodeling of the neurovascular unit. This finding suggests a specific effect of selegiline on the Notch-Jagged signaling in the penumbra. The upregulation of Notch-Jagged signaling is an important newly established effect of selegiline treatment, which has not been described before. The immune-histochemical investigations demonstrated an induction of Notch 1 and Jagged 1 at the protein level, thereby confirming our mRNA findings. Histology also provided additional spatial information on the induction

of the Notch-Jagged pathway. Notch 1- and Jagged 1–labeled cells appeared in the peri-infarct region, but not within the lesion in response to selegiline. Thus, selegiline further induced Notch 1 and Jagged 1 in the area where these genes already show elevated expression in response to ischemic insult. Notch 1 and Jagged 1 were induced by selegiline almost exclusively in astrocytes of the peri-infarct region, suggesting that selegiline enhances Notch-Jagged signaling in this cell type, thereby enhancing existent neurorestorative mechanisms. In view of the well-documented involvement of Notch-Jagged signaling in cell proliferation and activation, it is tempting to speculate that selegiline promotes the proliferation of reactive astrocytes and the re-establishment of the blood brain barrier following stroke through this signaling pathway. The upregulation of other astrocyte specific markers included in the array (Omg, Mog and Ptrz1) also seem to confirm this hypothesis.

It is interesting to note that selegiline is not the only drug with neurorestorative properties that increases Notch signaling. Simvastatin was also shown to increase Notch signaling and promote arterial-genesis after stroke (Zacharek et al., 2009). In addition, folic acid was demonstrated to enhance Notch signaling and cognitive function (learning and memory in Y-maze tests) following MCAO in rats (Zhang et al., 2012). Similarly, selegiline may also contribute to improved functional outcome following stroke, which awaits further investigation.

As selegiline activates astrocytes via the Notch pathway, it is expected to reduce edema based on the established role of reactive astrocytes. Indeed, we found decreased edema using MRI associated with selegiline treatment. In addition to the reinforcement of barrier function, the resorption of edema may be largely influenced by the microvascular network. Selegiline has been previously shown to exert a cytoprotective effect on human brain capillaries in vitro (Denes et al., 2006). Therefore, we decided to test its effect on the capillary network in vivo, following focal ischemia. Using RECA immunolabeling, we found an increased microvascular density in the peri-infarct region of the selegiline treated rats compared to controls. This effect is most likely not directly associated with Notch 1 signaling but is likely to contribute to the net beneficial impact of selegiline on neurovascular-unit integrity (Krupinski et al., 1994).

In addition to affecting the Notch pathway and microcirculation, selegiline also increased the expression of anti-apoptotic genes BCL XL and XIAP, confirming previous reports (Simon et al., 2001), which contributes to the validation of our data. As far as the mechanism of induction of anti-apoptotic genes, a direct effect of selegiline has been previously suggested (Simon et al., 2001; Tatton et al., 1994). Assuming the validity of these previous observations, the Bcl-2 family proteins may be the primary target of selegiline, which in turn induce Notch 1 activity as shown in thymic lymphoma cells (Sionov et al., 2012). It is clear, however, that a direct connection between the two pathways in the settings of cerebral ischemia/reperfusion remains to be established.

Because selegiline improves neurological function, we expected an upregulation in the markers of synaptic plasticity. In the case of the 9 investigated plasticity genes, however, we did not see any significant change induced by the therapy. When we interpret these negative results, it is important to note that our array provides only a snapshot of the dynamic interaction of genes following focal ischemia, and sampling at other time points of the post-stroke evolution may reveal a significantly different pattern of gene expression.

HIGHLIGHTS OF NEW FINDINGS

- We documented the upregulation of the Reticulon 4 receptor mRNA expression following gelatinase inhibition in the subacute phase of cerebral infarction in the peri-infarct cortex.
- Immunohistochemistry confirmed the increased Reticulon 4 receptor protein abundancy in the peri-infarct cortex following subacute gelatinase inhibitions.
- Double labeling confirmed that the upregulation of the Rtn4 receptor mainly involved the peri-infarct astrocytes, potentially suggesting increased glial scar formation.
- Selegiline treatment in the subacute phase of cerebral infarction induced the expression of Notch1 and Jagged mRNA in the peri-infarct region.
- Immunohistochemistry confirmed the increased Notch 1 and Jagged protein abundancy in the peri-infarct region in response to selegiline treatment.
- Double labeling showed the upregulation of the Notch1 and Jagged protein in astrocytes.
- Selegiline starting 2d after tMCAO reduced edema after 6d of treatment.
- Selegiline increased the density of capillary network in the peri-infarct region.

CONCLUSIONS

Improving the functional integrity of the blood brain barrier, without limiting the microvascular remodeling and neuronal plasticity is a very challenging, but very important task in developing future of stroke therapies. We experimentally tested two pharmacological interventions aimed at improving functional outcomes following large vessel occlusion.

While the inhibition of the acute MMP activity helped to preserve the neural tissue in previous stroke experiments, functional recovery was impaired by blocking the gelatinases in the delayed phase of stroke (Zhao et al., 2006). The known suppression of neurovascular remodeling, together with the currently documented increased number of Rtn4 receptor positive astrocytes in the peri-infarct cortex suggest, that the MMP – NOGO interaction may play an important role in post-stroke regeneration. Our data implicates, that an eventual prolonged inhibition of the gelatinases following cerebral infarction may risk to cause increased reactive gliosis, and therefore may interfere with functional recovery.

In the last few decades, hundreds of molecules were shown to induce recovery in animal models of cerebral infarction. However, most of these compounds did not prove to be clinically effective in humans (Endres et al., 2008). Selegiline, on the other hand, was shown to improve functional outcomes in stroke patients in a small randomized clinical trial (Sivenius et al., 2001). We therefore believe that the newly described beneficial effects on blood brain barrier function, together with the observed increase in microvascular density, may have further significance in stroke treatment.

SUMMARY

Emergent large vessel occlusions (ELVO) are defined by a proximal thrombotic blockage of the intra-cranial arteries, and without adequate treatment, they lead to poor functional outcomes and high mortality rate. Although mechanical thrombectomy represent a huge step forward in the treatment of this devastating disease, there remains a large demand for the development of new adjunctive therapies to improve the safety of revascularization and to offer alternative solutions for the reperfusion-non-eligible patients.

We used an array based method to analyze the mRNA expressional changes induced by two pharmacological interventions on a standard experimental model of ELVO. In previous experiments gelatinase inhibition was shown decrease bleeding transformation in the acute phase of the cerebral infarction, while in the subacute phase it worsened functional outcomes. Selegiline, a widely used compound in the treatment of Parkinson's disease was shown to exert neurorestorative action following stroke. The results of the gene expression study were confirmed by immunolabeling on the protein level.

The subacute gelatinase inhibition studied in our experiments caused a significant upregulation of the Reticulon 4 receptor expression of the astrocytes in the peri-infarct cortex, while selegiline treatment induced the expression of the Notch 1 receptor and its ligand Jagged 1 on the perilesional astrocytes besides a number of anti-apoptosis genes.

Although our findings suggest, that both studied pharmacological interventions influence reactive gliosis, the effect of selegiline was accompanied by a significant reduction of edema on MRI and an increased density of the capillary network, suggesting the restoration of physiological barriers. Gelatinase inhibition on the other hand is known to decrease microvascular remodeling in the subacute phase of stroke, therefore our results confirm the previously published observations that the proliferative effect of gelatinase inhibition on astrocytes is more likely to result in scar formation, than in neurorestorative action.

ÖSSZEFOGLALÁS

Az akut agyi nagyér okklúzió definíció szerint a koponyán belüli artériák proximális elzáródását jelenti, amely gyors ellátás hiányában maradandó neurológiai károsodáshoz és magas halálozási arányhoz vezethet. Bár a mechanikus trombektómia alkalmazása jelentős előrelépést jelent ezeknek a súlyos kórállapotoknak a kezelésében, továbbra is nagy szükség van olyan kiegészítő terápiás eljárások kifejlesztésére, amelyektől a revaszkularizáció biztonságosságának növekedése várható, illetve amelyek alternatív megoldást jelenthetnek a trombektómiára alkalmatlan betegek kezelése során.

Egy array alapú vizsgálat során tanulmányoztuk két gyógyszeres beavatkozás hatásait agyi nagyér okklúziós standard kisállat modelljén. A zselatináz enzim gátlása kísérletes körülmények között alkalmas volt a vérzéses transzformáció megelőzésére az agyi infarktus akut fázisában, míg a későbbi fázisban ugyanez a kezelés rontotta a neurológiai kimenetelt. A selegiline egy Parkinson kórban széles körben alkalmazott hatóanyag, amely irodalmi adatok alapján elősegítette a központi idegrendszer regenerációját agyi infarktust követően.

Kísérleteinkben a Reticulon 4 receptor expressziójának növekedését tapasztaltuk a peri-infarktusos agykéreg asztroglia sejtjeiben a szubakut zselatináz enzim gátlást követően, míg a selegiline kezelés mellett a reaktív asztrocitákon a Notch 1 receptor és ligandja a Jagged 1 expressziójának fokozódását dokumentáltuk, több anti-apoptózis gén fokozott kifejeződése mellett.

Az eredményeink alapján mindkét gyógyszeres kezelés befolyással van a reaktív asztrociták működésére, a selegiline kezelés hatása ugyanakkor együtt járt az infarktus körüli ödéma csökkenésével, és egy nagyobb sűrűségű kapilláris hálózat kialakulásával, ami a fiziológiás vér-agy gát regenerációjára utalhat. A zselatináz enzim gátlása ezzel szemben ismerten blokkolja az ér-újdonképződést, így ez utóbbi kezelés hatására inkább alakul ki a regenerációt gátló gliaheg semmint hatékonyan funkcionáló vér-agy gát.

REFERENCES

2009. in: Caplan, L. (Ed.), Caplan's Stroke: A Clinical Approach, 4th ed. Saunders Elsevier,, Philadelphia, p. 22.

Amantea, D., Corasaniti, M.T., Mercuri, N.B., Bernardi, G., Bagetta, G., 2008. Brain regional and cellular localization of gelatinase activity in rat that have undergone transient middle cerebral artery occlusion. *Neuroscience 152, 8-17.*

Ando, G., Capodanno, D., 2015. Radial Versus Femoral Access in Invasively Managed Patients With Acute Coronary Syndrome: A Systematic Review and Meta-analysis. *Annals of internal medicine 163, 932-940.*

Arumugam, T.V., Cheng, Y.L., Choi, Y., Choi, Y.H., Yang, S., Yun, Y.K., Park, J.S., Yang, D.K., Thundyil, J., Gelderblom, M., Karamyan, V.T., Tang, S.C., Chan, S.L., Magnus, T., Sobey, C.G., Jo, D.G., 2011. Evidence that gamma-secretase-mediated Notch signaling induces neuronal cell death via the nuclear factor-kappaB-Bcl-2-interacting mediator of cell death pathway in ischemic stroke. *Mol Pharmacol 80, 23-31.*

Asahi, M., Wang, X., Mori, T., Sumii, T., Jung, J.C., Moskowitz, M.A., Fini, M.E., Lo, E.H., 2001. Effects of matrix metalloproteinase-9 gene knock-out on the proteolysis of blood-brain barrier and white matter components after cerebral ischemia. *The Journal of neuroscience : the official journal of the Society for Neuroscience 21, 7724-7732.*

Bai, J., Lyden, P.D., 2015. Revisiting cerebral postischemic reperfusion injury: new insights in understanding reperfusion failure, hemorrhage, and edema. *International journal of stroke : official journal of the International Stroke Society 10, 143-152.*

Beck, H., Plate, K.H., 2009. Angiogenesis after cerebral ischemia. *Acta neuropathologica 117, 481-496.*

Benowitz, L.I., Goldberg, D.E., Irwin, N., 2002. Inosine stimulates axon growth in vitro and in the adult CNS. *Progress in brain research 137, 389-399.*

Berkhemer, O.A., Fransen, P.S., Beumer, D., van den Berg, L.A., Lingsma, H.F., Yoo, A.J., Schonewille, W.J., Vos, J.A., Nederkoorn, P.J., Wermer, M.J., van Walderveen, M.A., Staals, J., Hofmeijer, J., van Oostayen, J.A., Lycklama a Nijeholt, G.J., Boiten, J., Brouwer,

P.A., Emmer, B.J., de Bruijn, S.F., van Dijk, L.C., Kappelle, L.J., Lo, R.H., van Dijk, E.J., de Vries, J., de Kort, P.L., van Rooij, W.J., van den Berg, J.S., van Hasselt, B.A., Aerden, L.A., Dallinga, R.J., Visser, M.C., Bot, J.C., Vroomen, P.C., Eshghi, O., Schreuder, T.H., Heijboer, R.J., Keizer, K., Tielbeek, A.V., den Hertog, H.M., Gerrits, D.G., van den Berg-Vos, R.M., Karas, G.B., Steyerberg, E.W., Flach, H.Z., Marquering, H.A., Sprengers, M.E., Jenniskens, S.F., Beenen, L.F., van den Berg, R., Koudstaal, P.J., van Zwam, W.H., Roos, Y.B., van der Lugt, A., van Oostenbrugge, R.J., Majoie, C.B., Dippel, D.W., 2015. A randomized trial of intraarterial treatment for acute ischemic stroke. *The New England journal of medicine 372, 11-20.*

Bomze, H.M., Bulsara, K.R., Iskandar, B.J., Caroni, P., Skene, J.H., 2001. Spinal axon regeneration evoked by replacing two growth cone proteins in adult neurons. *Nature neuroscience 4, 38-43.*

Broderick, J.P., Palesch, Y.Y., Demchuk, A.M., Yeatts, S.D., Khatri, P., Hill, M.D., Jauch, E.C., Jovin, T.G., Yan, B., Silver, F.L., von Kummer, R., Molina, C.A., Demaerschalk, B.M., Budzik, R., Clark, W.M., Zaidat, O.O., Malisch, T.W., Goyal, M., Schonewille, W.J., Mazighi, M., Engelter, S.T., Anderson, C., Spilker, J., Carrozzella, J., Ryckborst, K.J., Janis, L.S., Martin, R.H., Foster, L.D., Tomsick, T.A., 2013. Endovascular therapy after intravenous t-PA versus t-PA alone for stroke. *The New England journal of medicine 368, 893-903.*

Broughton, B.R., Reutens, D.C., Sobey, C.G., 2009. Apoptotic mechanisms after cerebral ischemia. *Stroke; a journal of cerebral circulation 40, e331-339.*

Burggraf, D., Martens, H.K., Dichgans, M., Hamann, G.F., 2007. Matrix metalloproteinase (MMP) induction and inhibition at different doses of recombinant tissue plasminogen activator following experimental stroke. *Thromb Haemost 98, 963-969.*

Bush, T.G., Puvanachandra, N., Horner, C.H., Polito, A., Ostenfeld, T., Svendsen, C.N., Mucke, L., Johnson, M.H., Sofroniew, M.V., 1999. Leukocyte infiltration, neuronal degeneration, and neurite outgrowth after ablation of scar-forming, reactive astrocytes in adult transgenic mice. *Neuron 23, 297-308.*

Calautti, C., Baron, J.C., 2003. Functional neuroimaging studies of motor recovery after stroke in adults: a review. *Stroke; a journal of cerebral circulation 34, 1553-1566.*

Campbell, B.C., Mitchell, P.J., Kleinig, T.J., Dewey, H.M., Churilov, L., Yassi, N., Yan, B., Dowling, R.J., Parsons, M.W., Oxley, T.J., Wu, T.Y., Brooks, M., Simpson, M.A., Miteff, F., Levi, C.R., Krause, M., Harrington, T.J., Faulder, K.C., Steinfort, B.S., Priglinger, M., Ang, T., Scroop, R., Barber, P.A., McGuinness, B., Wijeratne, T., Phan, T.G., Chong, W., Chandra, R.V., Bladin, C.F., Badve, M., Rice, H., de Villiers, L., Ma, H., Desmond, P.M., Donnan, G.A., Davis, S.M., 2015. Endovascular therapy for ischemic stroke with perfusion-imaging selection. *The New England journal of medicine 372, 1009-1018.*

Carmichael, S.T., 2003. Gene expression changes after focal stroke, traumatic brain and spinal cord injuries. *Current opinion in neurology 16, 699-704.*

Carmichael, S.T., Archibeque, I., Luke, L., Nolan, T., Momiy, J., Li, S., 2005. Growth-associated gene expression after stroke: evidence for a growth-promoting region in peri-infarct cortex. *Experimental neurology 193, 291-311.*

Christou, I., Burgin, W.S., Alexandrov, A.V., Grotta, J.C., 2001. Arterial status after intravenous TPA therapy for ischaemic stroke. A need for further interventions. *International angiology : a journal of the International Union of Angiology 20, 208-213.*

Clegg, L.E., Mac Gabhann, F., 2015. Systems biology of the microvasculature. *Integrative biology : quantitative biosciences from nano to macro 7, 498-512.*

Dalkara, T., Arsava, E.M., 2012. Can restoring incomplete microcirculatory reperfusion improve stroke outcome after thrombolysis? *Journal of cerebral blood flow and metabolism : official journal of the International Society of Cerebral Blood Flow and Metabolism 32, 2091-2099.*

del Zoppo, G.J., 2009. Inflammation and the neurovascular unit in the setting of focal cerebral ischemia. *Neuroscience 158, 972-982.*

Demestre, M., Wells, G.M., Miller, K.M., Smith, K.J., Hughes, R.A., Gearing, A.J., Gregson, N.A., 2004. Characterisation of matrix metalloproteinases and the effects of a broad-spectrum inhibitor (BB-1101) in peripheral nerve regeneration. *Neuroscience 124, 767-779.*

Denes, L., Szilagyi, G., Gal, A., Bori, Z., Nagy, Z., 2006. Cytoprotective effect of two synthetic enhancer substances, (-)-BPAP and (-)-deprenyl, on human brain capillary endothelial cells and rat PC12 cells. *Life Sci 79, 1034-1039.*

Derdeyn, C.P., Chimowitz, M.I., Lynn, M.J., Fiorella, D., Turan, T.N., Janis, L.S., Montgomery, J., Nizam, A., Lane, B.F., Lutsep, H.L., Barnwell, S.L., Waters, M.F., Hoh, B.L., Hourihane, J.M., Levy, E.I., Alexandrov, A.V., Harrigan, M.R., Chiu, D., Klucznik, R.P., Clark, J.M., McDougall, C.G., Johnson, M.D., Pride, G.L., Jr., Lynch, J.R., Zaidat, O.O., Rumboldt, Z., Cloft, H.J., 2014. Aggressive medical treatment with or without stenting in high-risk patients with intracranial artery stenosis (SAMMPRIS): the final results of a randomised trial. *Lancet (London, England) 383, 333-341.*

Elkins, P.A., Ho, Y.S., Smith, W.W., Janson, C.A., D'Alessio, K.J., McQueney, M.S., Cummings, M.D., Romanic, A.M., 2002. Structure of the C-terminally truncated human ProMMP9, a gelatin-binding matrix metalloproteinase. *Acta crystallographica. Section D, Biological crystallography 58, 1182-1192.*

Emberson, J., Lees, K.R., Lyden, P., Blackwell, L., Albers, G., Bluhmki, E., Brott, T., Cohen, G., Davis, S., Donnan, G., Grotta, J., Howard, G., Kaste, M., Koga, M., von Kummer, R., Lansberg, M., Lindley, R.I., Murray, G., Olivot, J.M., Parsons, M., Tilley, B., Toni, D., Toyoda, K., Wahlgren, N., Wardlaw, J., Whiteley, W., del Zoppo, G.J., Baigent, C., Sandercock, P., Hacke, W., 2014. Effect of treatment delay, age, and stroke severity on the effects of intravenous thrombolysis with alteplase for acute ischaemic stroke: a meta-analysis of individual patient data from randomised trials. *Lancet (London, England) 384, 1929-1935.*

Endres, M., Engelhardt, B., Koistinaho, J., Lindvall, O., Meairs, S., Mohr, J.P., Planas, A., Rothwell, N., Schwaninger, M., Schwab, M.E., Vivien, D., Wieloch, T., Dirnagl, U., 2008. Improving outcome after stroke: overcoming the translational roadblock. *Cerebrovasc Dis 25, 268-278.*

Feigin, V.L., Forouzanfar, M.H., Krishnamurthi, R., Mensah, G.A., Connor, M., Bennett, D.A., Moran, A.E., Sacco, R.L., Anderson, L., Truelsen, T., O'Donnell, M., Venketasubramanian, N., Barker-Collo, S., Lawes, C.M., Wang, W., Shinohara, Y., Witt, E., Ezzati, M., Naghavi, M., Murray, C., 2014. Global and regional burden of stroke during

1990-2010: findings from the Global Burden of Disease Study 2010. *Lancet (London, England) 383, 245-254.*

Fransen, P.S., Berkhemer, O.A., Lingsma, H.F., Beumer, D., van den Berg, L.A., Yoo, A.J., Schonewille, W.J., Vos, J.A., Nederkoorn, P.J., Wermer, M.J., van Walderveen, M.A., Staals, J., Hofmeijer, J., van Oostayen, J.A., Lycklama, A.N.G.J., Boiten, J., Brouwer, P.A., Emmer, B.J., de Bruijn, S.F., van Dijk, L.C., Kappelle, L.J., Lo, R.H., van Dijk, E.J., de Vries, J., de Kort, P.L., van den Berg, J.S., van Hasselt, B.A., Aerden, L.A., Dallinga, R.J., Visser, M.C., Bot, J.C., Vroomen, P.C., Eshghi, O., Schreuder, T.H., Heijboer, R.J., Keizer, K., Tielbeek, A.V., den Hertog, H.M., Gerrits, D.G., van den Berg-Vos, R.M., Karas, G.B., Steyerberg, E.W., Flach, H.Z., Marquering, H.A., Sprengers, M.E., Jenniskens, S.F., Beenen, L.F., van den Berg, R., Koudstaal, P.J., van Zwam, W.H., Roos, Y.B., van Oostenbrugge, R.J., Majoie, C.B., van der Lugt, A., Dippel, D.W., 2016. Time to Reperfusion and Treatment Effect for Acute Ischemic Stroke: A Randomized Clinical Trial. *JAMA neurology 73, 190-196.*

Funahashi, S., Hasegawa, T., Nagano, A., Sato, K., 2008. Differential expression patterns of messenger RNAs encoding Nogo receptors and their ligands in the rat central nervous system. *The Journal of comparative neurology 506, 141-160.*

Ginsberg, M.D., 1997. The new language of cerebral ischemia. *AJNR. American journal of neuroradiology 18, 1435-1445.*

Goyal, M., Demchuk, A.M., Menon, B.K., Eesa, M., Rempel, J.L., Thornton, J., Roy, D., Jovin, T.G., Willinsky, R.A., Sapkota, B.L., Dowlatshahi, D., Frei, D.F., Kamal, N.R., Montanera, W.J., Poppe, A.Y., Ryckborst, K.J., Silver, F.L., Shuaib, A., Tampieri, D., Williams, D., Bang, O.Y., Baxter, B.W., Burns, P.A., Choe, H., Heo, J.H., Holmstedt, C.A., Jankowitz, B., Kelly, M., Linares, G., Mandzia, J.L., Shankar, J., Sohn, S.I., Swartz, R.H., Barber, P.A., Coutts, S.B., Smith, E.E., Morrish, W.F., Weill, A., Subramaniam, S., Mitha, A.P., Wong, J.H., Lowerison, M.W., Sajobi, T.T., Hill, M.D., 2015. Randomized assessment of rapid endovascular treatment of ischemic stroke. *The New England journal of medicine 372, 1019-1030.*

Goyal, M., Menon, B.K., van Zwam, W.H., Dippel, D.W., Mitchell, P.J., Demchuk, A.M., Davalos, A., Majoie, C.B., van der Lugt, A., de Miquel, M.A., Donnan, G.A., Roos, Y.B.,

Bonafe, A., Jahan, R., Diener, H.C., van den Berg, L.A., Levy, E.I., Berkhemer, O.A., Pereira, V.M., Rempel, J., Millan, M., Davis, S.M., Roy, D., Thornton, J., Roman, L.S., Ribo, M., Beumer, D., Stouch, B., Brown, S., Campbell, B.C., van Oostenbrugge, R.J., Saver, J.L., Hill, M.D., Jovin, T.G., 2016. Endovascular thrombectomy after large-vessel ischaemic stroke: a meta-analysis of individual patient data from five randomised trials. *Lancet (London, England).*

GrandPre, T., Li, S., Strittmatter, S.M., 2002. Nogo-66 receptor antagonist peptide promotes axonal regeneration. *Nature 417, 547-551.*

Guo, F., Lv, S., Lou, Y., Tu, W., Liao, W., Wang, Y., Deng, Z., 2012. Bone marrow stromal cells enhance the angiogenesis in ischaemic cortex after stroke: involvement of notch signalling. *Cell Biol Int 36, 997-1004.*

Hacke, W., Schwab, S., Horn, M., Spranger, M., De Georgia, M., von Kummer, R., 1996. 'Malignant' middle cerebral artery territory infarction: clinical course and prognostic signs. *Archives of neurology 53, 309-315.*

Hansen, C.K., Christensen, A., Ovesen, C., Havsteen, I., Christensen, H., 2015. Stroke severity and incidence of acute large vessel occlusions in patients with hyper-acute cerebral ischemia: results from a prospective cohort study based on CT-angiography (CTA). *International journal of stroke : official journal of the International Stroke Society 10, 336-342.*

Hayashita-Kinoh, H., Kinoh, H., Okada, A., Komori, K., Itoh, Y., Chiba, T., Kajita, M., Yana, I., Seiki, M., 2001. Membrane-type 5 matrix metalloproteinase is expressed in differentiated neurons and regulates axonal growth. *Cell Growth Differ 12, 573-580.*

Irvin, D.K., Nakano, I., Paucar, A., Kornblum, H.I., 2004. Patterns of Jagged1, Jagged2, Delta-like 1 and Delta-like 3 expression during late embryonic and postnatal brain development suggest multiple functional roles in progenitors and differentiated cells. *J Neurosci Res 75, 330-343.*

Irvin, D.K., Zurcher, S.D., Nguyen, T., Weinmaster, G., Kornblum, H.I., 2001. Expression patterns of Notch1, Notch2, and Notch3 suggest multiple functional roles for the Notch-DSL signaling system during brain development. *The Journal of comparative neurology 436, 167-181.*

Jauch, E.C., Saver, J.L., Adams, H.P., Jr., Bruno, A., Connors, J.J., Demaerschalk, B.M., Khatri, P., McMullan, P.W., Jr., Qureshi, A.I., Rosenfield, K., Scott, P.A., Summers, D.R., Wang, D.Z., Wintermark, M., Yonas, H., 2013. Guidelines for the early management of patients with acute ischemic stroke: a guideline for healthcare professionals from the American Heart Association/American Stroke Association. *Stroke; a journal of cerebral circulation 44, 870-947.*

Jovin, T.G., Chamorro, A., Cobo, E., de Miquel, M.A., Molina, C.A., Rovira, A., San Roman, L., Serena, J., Abilleira, S., Ribo, M., Millan, M., Urra, X., Cardona, P., Lopez-Cancio, E., Tomasello, A., Castano, C., Blasco, J., Aja, L., Dorado, L., Quesada, H., Rubiera, M., Hernandez-Perez, M., Goyal, M., Demchuk, A.M., von Kummer, R., Gallofre, M., Davalos, A., 2015. Thrombectomy within 8 hours after symptom onset in ischemic stroke. *The New England journal of medicine 372, 2296-2306.*

Kidwell, C.S., Jahan, R., Saver, J.L., 2013. Endovascular treatment for acute ischemic stroke. *The New England journal of medicine 368, 2434-2435.*

Knoll, J., Ecsery, Z., Magyar, K., Satory, E., 1978. Novel (-)deprenyl-derived selective inhibitors of B-type monoamine oxidase. The relation of structure to their action. *Biochemical pharmacology 27, 1739-1747.*

Krishnamurthi, R.V., Feigin, V.L., Forouzanfar, M.H., Mensah, G.A., Connor, M., Bennett, D.A., Moran, A.E., Sacco, R.L., Anderson, L.M., Truelsen, T., O'Donnell, M., Venketasubramanian, N., Barker-Collo, S., Lawes, C.M., Wang, W., Shinohara, Y., Witt, E., Ezzati, M., Naghavi, M., Murray, C., 2013. Global and regional burden of first-ever ischaemic and haemorrhagic stroke during 1990-2010: findings from the Global Burden of Disease Study 2010. *The Lancet. Global health 1, e259-281.*

Krupinski, J., Kaluza, J., Kumar, P., Kumar, S., Wang, J.M., 1994. Role of angiogenesis in patients with cerebral ischemic stroke. *Stroke; a journal of cerebral circulation 25, 1794-1798.*

Krupinski, J., Stroemer, P., Slevin, M., Marti, E., Kumar, P., Rubio, F., 2003. Three-dimensional structure and survival of newly formed blood vessels after focal cerebral ischemia. *Neuroreport 14, 1171-1176.*

Lansberg, M.G., O'Donnell, M.J., Khatri, P., Lang, E.S., Nguyen-Huynh, M.N., Schwartz, N.E., Sonnenberg, F.A., Schulman, S., Vandvik, P.O., Spencer, F.A., Alonso-Coello, P., Guyatt, G.H., Akl, E.A., 2012. Antithrombotic and thrombolytic therapy for ischemic stroke: Antithrombotic Therapy and Prevention of Thrombosis, 9th ed: American College of Chest Physicians Evidence-Based Clinical Practice Guidelines. *Chest 141, e601S-636S.*

Laux, T., Fukami, K., Thelen, M., Golub, T., Frey, D., Caroni, P., 2000. GAP43, MARCKS, and CAP23 modulate PI(4,5)P(2) at plasmalemmal rafts, and regulate cell cortex actin dynamics through a common mechanism. *The Journal of cell biology 149, 1455-1472.*

Lee, H.S., Han, J., Bai, H.J., Kim, K.W., 2009. Brain angiogenesis in developmental and pathological processes: regulation, molecular and cellular communication at the neurovascular interface. *The FEBS journal 276, 4622-4635.*

Lee, S.R., Lo, E.H., 2004. Induction of caspase-mediated cell death by matrix metalloproteinases in cerebral endothelial cells after hypoxia-reoxygenation. *Journal of cerebral blood flow and metabolism : official journal of the International Society of Cerebral Blood Flow and Metabolism 24, 720-727.*

Li, L., Lundkvist, A., Andersson, D., Wilhelmsson, U., Nagai, N., Pardo, A.C., Nodin, C., Stahlberg, A., Aprico, K., Larsson, K., Yabe, T., Moons, L., Fotheringham, A., Davies, I., Carmeliet, P., Schwartz, J.P., Pekna, M., Kubista, M., Blomstrand, F., Maragakis, N., Nilsson, M., Pekny, M., 2008. Protective role of reactive astrocytes in brain ischemia. *Journal of cerebral blood flow and metabolism : official journal of the International Society of Cerebral Blood Flow and Metabolism 28, 468-481.*

Lima, F.O., Furie, K.L., Silva, G.S., Lev, M.H., Camargo, E.C., Singhal, A.B., Harris, G.J., Halpern, E.F., Koroshetz, W.J., Smith, W.S., Nogueira, R.G., 2014. Prognosis of untreated strokes due to anterior circulation proximal intracranial arterial occlusions detected by use of computed tomography angiography. *JAMA neurology 71, 151-157.*

Longa, E.Z., Weinstein, P.R., Carlson, S., Cummins, R., 1989. Reversible middle cerebral artery occlusion without craniectomy in rats. *Stroke; a journal of cerebral circulation 20, 84-91.*

Love, S., 2003. Apoptosis and brain ischaemia. *Progress in neuro-psychopharmacology & biological psychiatry 27, 267-282.*

Malmivaara, A., Meretoja, A., Peltola, M., Numerato, D., Heijink, R., Engelfriet, P., Wild, S.H., Belicza, E., Bereczki, D., Medin, E., Goude, F., Boncoraglio, G., Tatlisumak, T., Seppala, T., Hakkinen, U., 2015. Comparing ischaemic stroke in six European countries. The EuroHOPE register study. *European journal of neurology 22, 284-291, e225-286.*

Nardai, S., Dobolyi, A., Pal, G., Skopal, J., Pinter, N., Lakatos, K., Merkely, B., Nagy, Z., 2015. Selegiline promotes NOTCH-JAGGED signaling in astrocytes of the peri-infarct region and improves the functional integrity of the neurovascular unit in a rat model of focal ischemia. *Restorative neurology and neuroscience 33, 1-14.*

Nardai, S., Dobolyi, A., Skopal, J., Lakatos, K., Merkely, B., Nagy, Z., 2016. Delayed Gelatinase Inhibition Induces Reticulon 4 Receptor Expression in the Peri-Infarct Cortex. *JOURNAL OF NEUROPATHOLOGY AND EXPERIMENTAL NEUROLOGY 75, 379-385.*

Oh, L.Y., Larsen, P.H., Krekoski, C.A., Edwards, D.R., Donovan, F., Werb, Z., Yong, V.W., 1999. Matrix metalloproteinase-9/gelatinase B is required for process outgrowth by oligodendrocytes. *The Journal of neuroscience : the official journal of the Society for Neuroscience 19, 8464-8475.*

Opdenakker, G., Van den Steen, P.E., Dubois, B., Nelissen, I., Van Coillie, E., Masure, S., Proost, P., Van Damme, J., 2001. Gelatinase B functions as regulator and effector in leukocyte biology. *J Leukoc Biol 69, 851-859.*

Oya, S., Yoshikawa, G., Takai, K., Tanaka, J.I., Higashiyama, S., Saito, N., Kirino, T., Kawahara, N., 2009. Attenuation of Notch signaling promotes the differentiation of neural progenitors into neurons in the hippocampal CA1 region after ischemic injury. *Neuroscience 158, 683-692.*

Pavlidis, P., Li, Q., Noble, W.S., 2003. The effect of replication on gene expression microarray experiments. *Bioinformatics 19, 1620-1627.*

Pekny, M., Wilhelmsson, U., Pekna, M., 2014. The dual role of astrocyte activation and reactive gliosis. *Neurosci Lett 565c, 30-38.*

Powers, W.J., Derdeyn, C.P., Biller, J., Coffey, C.S., Hoh, B.L., Jauch, E.C., Johnston, K.C., Johnston, S.C., Khalessi, A.A., Kidwell, C.S., Meschia, J.F., Ovbiagele, B., Yavagal,

D.R., 2015. 2015 American Heart Association/American Stroke Association Focused Update of the 2013 Guidelines for the Early Management of Patients With Acute Ischemic Stroke Regarding Endovascular Treatment: A Guideline for Healthcare Professionals From the American Heart Association/American Stroke Association. *Stroke; a journal of cerebral circulation 46, 3020-3035.*

Puurunen, K., Jolkkonen, J., Sirvio, J., Haapalinna, A., Sivenius, J., 2001. Selegiline combined with enriched-environment housing attenuates spatial learning deficits following focal cerebral ischemia in rats. *Experimental neurology 167, 348-355.*

Quaegebeur, A., Lange, C., Carmeliet, P., 2011. The neurovascular link in health and disease: molecular mechanisms and therapeutic implications. *Neuron 71, 406-424.*

Ridet, J.L., Malhotra, S.K., Privat, A., Gage, F.H., 1997. Reactive astrocytes: cellular and molecular cues to biological function. *Trends Neurosci 20, 570-577.*

Risau, W., 1997. Mechanisms of angiogenesis. *Nature 386, 671-674.*

Ruzsa, Z., Nemes, B., Pinter, L., Berta, B., Toth, K., Teleki, B., Nardai, S., Jambrik, Z., Szabo, G., Kolvenbach, R., Huttl, K., Merkely, B., 2014. A randomised comparison of transradial and transfemoral approach for carotid artery stenting: RADCAR (RADial access for CARotid artery stenting) study. *EuroIntervention : journal of EuroPCR in collaboration with the Working Group on Interventional Cardiology of the European Society of Cardiology 10, 381-391.*

Sandercock, P.A., Counsell, C., Kane, E.J., 2015. Anticoagulants for acute ischaemic stroke. *The Cochrane database of systematic reviews 3, Cd000024.*

Saver, J.L., Goyal, M., Bonafe, A., Diener, H.C., Levy, E.I., Pereira, V.M., Albers, G.W., Cognard, C., Cohen, D.J., Hacke, W., Jansen, O., Jovin, T.G., Mattle, H.P., Nogueira, R.G., Siddiqui, A.H., Yavagal, D.R., Baxter, B.W., Devlin, T.G., Lopes, D.K., Reddy, V.K., du Mesnil de Rochemont, R., Singer, O.C., Jahan, R., 2015. Stent-retriever thrombectomy after intravenous t-PA vs. t-PA alone in stroke. *The New England journal of medicine 372, 2285-2295.*

Shimada, I.S., Borders, A., Aronshtam, A., Spees, J.L., 2011. Proliferating reactive astrocytes are regulated by Notch-1 in the peri-infarct area after stroke. *Stroke; a journal of cerebral circulation 42, 3231-3237.*

Simon, L., Szilagyi, G., Bori, Z., Orbay, P., Nagy, Z., 2001. (-)-D-Deprenyl attenuates apoptosis in experimental brain ischaemia. *European journal of pharmacology 430, 235-241.*

Simon, L., Szilagyi, G., Bori, Z., Telek, G., Magyar, K., Nagy, Z., 2005. Low dose (-)deprenyl is cytoprotective: it maintains mitochondrial membrane potential and eliminates oxygen radicals. *Life sciences 78, 225-231.*

Sionov, R.V., Kfir-Erenfeld, S., Spokoini, R., Yefenof, E., 2012. A role for bcl-2 in notch1-dependent transcription in thymic lymphoma cells. *Adv Hematol 2012, 435241.*

Sivenius, J., Sarasoja, T., Aaltonen, H., Heinonen, E., Kilkku, O., Reinikainen, K., 2001. Selegiline treatment facilitates recovery after stroke. *Neurorehabil Neural Repair 15, 183-190.*

Staykov, D., Gupta, R., 2011. Hemicraniectomy in malignant middle cerebral artery infarction. *Stroke; a journal of cerebral circulation 42, 513-516.*

Stump, G., Durrer, A., Klein, A.L., Lutolf, S., Suter, U., Taylor, V., 2002. Notch1 and its ligands Delta-like and Jagged are expressed and active in distinct cell populations in the postnatal mouse brain. *Mech Dev 114, 153-159.*

Sugawara, T., Fujimura, M., Noshita, N., Kim, G.W., Saito, A., Hayashi, T., Narasimhan, P., Maier, C.M., Chan, P.H., 2004. Neuronal death/survival signaling pathways in cerebral ischemia. *NeuroRx : the journal of the American Society for Experimental NeuroTherapeutics 1, 17-25.*

Szilagyi, G., Simon, L., Wappler, E., Magyar, K., Nagy, Z., 2009. (-)Deprenyl-N-oxide, a (-)deprenyl metabolite, is cytoprotective after hypoxic injury in PC12 cells, or after transient brain ischemia in gerbils. *Journal of the neurological sciences 283, 182-186.*

Tan, S., Wang, D., Liu, M., Zhang, S., Wu, B., Liu, B., 2014. Frequency and predictors of spontaneous hemorrhagic transformation in ischemic stroke and its association with prognosis. *Journal of neurology 261, 905-912.*

Tatton, W.G., Ju, W.Y., Holland, D.P., Tai, C., Kwan, M., 1994. (-)-Deprenyl reduces PC12 cell apoptosis by inducing new protein synthesis. *J Neurochem 63, 1572-1575.*

Unal-Cevik, I., Kilinc, M., Gursoy-Ozdemir, Y., Gurer, G., Dalkara, T., 2004. Loss of NeuN immunoreactivity after cerebral ischemia does not indicate neuronal cell loss: a cautionary note. *Brain research 1015, 169-174.*

van Swieten, J.C., Koudstaal, P.J., Visser, M.C., Schouten, H.J., van Gijn, J., 1988. Interobserver agreement for the assessment of handicap in stroke patients. *Stroke; a journal of cerebral circulation 19, 604-607.*

Wahlgren, N., Moreira, T., Michel, P., Steiner, T., Jansen, O., Cognard, C., Mattle, H.P., van Zwam, W., Holmin, S., Tatlisumak, T., Petersson, J., Caso, V., Hacke, W., Mazighi, M., Arnold, M., Fischer, U., Szikora, I., Pierot, L., Fiehler, J., Gralla, J., Fazekas, F., Lees, K.R., 2016. Mechanical thrombectomy in acute ischemic stroke: Consensus statement by ESO-Karolinska Stroke Update 2014/2015, supported by ESO, ESMINT, ESNR and EAN. *International journal of stroke : official journal of the International Stroke Society 11, 134-147.*

Walmsley, A.R., McCombie, G., Neumann, U., Marcellin, D., Hillenbrand, R., Mir, A.K., Frentzel, S., 2004. Zinc metalloproteinase-mediated cleavage of the human Nogo-66 receptor. *J Cell Sci 117, 4591-4602.*

Wang, B., Xiao, Z., Chen, B., Han, J., Gao, Y., Zhang, J., Zhao, W., Wang, X., Dai, J., 2008. Nogo-66 promotes the differentiation of neural progenitors into astroglial lineage cells through mTOR-STAT3 pathway. *PloS one 3, e1856.*

Wang, L., Chopp, M., Zhang, R.L., Zhang, L., Letourneau, Y., Feng, Y.F., Jiang, A., Morris, D.C., Zhang, Z.G., 2009. The Notch pathway mediates expansion of a progenitor pool and neuronal differentiation in adult neural progenitor cells after stroke. *Neuroscience 158, 1356-1363.*

Webster, K.A., Graham, R.M., Thompson, J.W., Spiga, M.G., Frazier, D.P., Wilson, A., Bishopric, N.H., 2006. Redox stress and the contributions of BH3-only proteins to infarction. *Antioxidants & redox signaling 8, 1667-1676.*

Wei, Z., Chigurupati, S., Arumugam, T.V., Jo, D.G., Li, H., Chan, S.L., 2011. Notch activation enhances the microglia-mediated inflammatory response associated with focal cerebral ischemia. *Stroke; a journal of cerebral circulation 42, 2589-2594.*

White, R.E., Jakeman, L.B., 2008. Don't fence me in: harnessing the beneficial roles of astrocytes for spinal cord repair. *Restorative neurology and neuroscience 26, 197-214.*

Wouters, A., Lemmens, R., Christensen, S., Wilms, G., Dupont, P., Mlynash, M., Schneider, A., Laage, R., Cereda, C.W., Lansberg, M.G., Albers, G.W., Thijs, V., 2016. Magnetic resonance imaging-based endovascular versus medical stroke treatment for symptom onset up to 12 h. *International journal of stroke : official journal of the International Stroke Society 11, 127-133.*

Yang, G.Y., Betz, A.L., 1994. Reperfusion-induced injury to the blood-brain barrier after middle cerebral artery occlusion in rats. *Stroke; a journal of cerebral circulation 25, 1658-1664; discussion 1664-1655.*

Yang, Y., Estrada, E.Y., Thompson, J.F., Liu, W., Rosenberg, G.A., 2007. Matrix metalloproteinase-mediated disruption of tight junction proteins in cerebral vessels is reversed by synthetic matrix metalloproteinase inhibitor in focal ischemia in rat. *Journal of cerebral blood flow and metabolism : official journal of the International Society of Cerebral Blood Flow and Metabolism 27, 697-709.*

Yuan, C.C., Peterson, R.J., Wang, C.D., Goodsaid, F., Waters, D.J., 2000. 5' Nuclease assays for the loci CCR5-+/Delta32, CCR2-V64I, and SDF1-G801A related to pathogenesis of AIDS. *Clinical chemistry 46, 24-30.*

Zacharek, A., Chen, J., Cui, X., Yang, Y., Chopp, M., 2009. Simvastatin increases notch signaling activity and promotes arteriogenesis after stroke. *Stroke; a journal of cerebral circulation 40, 254-260.*

Zhang, X., Huang, G., Liu, H., Chang, H., Wilson, J.X., 2012. Folic acid enhances Notch signaling, hippocampal neurogenesis, and cognitive function in a rat model of cerebral ischemia. *Nutr Neurosci 15, 55-61.*

Zhao, B.Q., Wang, S., Kim, H.Y., Storrie, H., Rosen, B.R., Mooney, D.J., Wang, X., Lo, E.H., 2006. Role of matrix metalloproteinases in delayed cortical responses after stroke. *Nat Med 12, 441-445.*

ZhuGe, Q., Zhong, M., Zheng, W., Yang, G.Y., Mao, X., Xie, L., Chen, G., Chen, Y., Lawton, M.T., Young, W.L., Greenberg, D.A., Jin, K., 2009. Notch-1 signalling is activated in brain arteriovenous malformations in humans. *Brain 132, 3231-3241.*

Zinkstok, S.M., Roos, Y.B., 2012. Early administration of aspirin in patients treated with alteplase for acute ischaemic stroke: a randomised controlled trial. *Lancet (London, England) 380, 731-737.*

LIST OF PUBLICATIONS

Publications related to the doctoral thesis

1. Nardai S , Dobolyi A , Skopal J , Lakatos K , Merkely B , Nagy Z
   Delayed Gelatinase Inhibition Induces Reticulon 4 Receptor Expression in the Peri-Infarct Cortex.
   JOURNAL OF NEUROPATHOLOGY AND EXPERIMENTAL NEUROLOGY 75:(4) pp. 379-385. (2016) **IF:3,8**

2. Nardai S , Dobolyi A , Pal G , Skopal J , Pinter N , Lakatos K , Merkely B , Nagy Z
   Selegiline promotes NOTCH-JAGGED signaling in astrocytes of the peri-infarct region and improves the functional integrity of the neurovascular unit in a rat model of focal ischemia.
   RESTORATIVE NEUROLOGY AND NEUROSCIENCE 33:(1) pp. 1-14. (2015) **IF:2,5**
   Independent citation: 2, self-citation: 1

3. Ruzsa Z , Nemes B , Pinter L , Berta B , Toth K , Teleki B , Nardai S , Jambrik Z , Szabo G , Kolvenbach R , Huttl K , Merkely B
   A randomised comparison of transradial and transfemoral approach for carotid artery stenting: RADCAR (RADial access for CARotid artery stenting) study
   EUROINTERVENTION 10:(3) pp. 381-391. (2014) **IF: 3,8**
   Independent citation: 4, self-citation : 1

Other original publications:

1 Ruzsa Z , Edes IF , Nardai S , Tóth K, Nemes B, Merkely B
Transradial and transulnar access for iliac artery interventions using sheathless guiding systems: a feasibility study.
CATHETERIZATION AND CARDIOVASCULAR INTERVENTIONS [Epub ahead of print] 2016. **IF:2,1**

2 Kolossváry M , Szilveszter B , Édes IF, Nardai S , Vörös V, Hartyánszky I, Merkely B, Voros S, Maurovich-Horvath P.
Comparison of Quantity of Coronary Atherosclerotic Plaques Detected by Computed Tomography Versus Angiography
AMERICAN JOURNAL OF CARDIOLOGY 2016 Apr 5. doi: 10.1016/j.amjcard.2016.03.031. [Epub ahead of print] **IF:3.3**

3. Edes IF , Ruzsa Z , Szabo G , Nardai S , Becker D , Benke K , Szilveszter B , Merkely B
   Clinical predictors of mortality following rotational atherectomy and stent implantation in high-risk patients: A single center experience.
   CATHETERIZATION AND CARDIOVASCULAR INTERVENTIONS 86:(4) pp. 634-641. (2015) Independent citation: 3 **IF:2,1**

4. Ruzsa Z , Toth K , Jambrik Z , Kovacs N , Nardai S , Nemes B , Huttl K , Merkely B
   Transradial access for renal artery intervention
   INTERVENTIONAL MEDICINE AND APPLIED SCIENCE 6:(3) pp. 97-103. (2014)
   Independent citation: 3

Citable International abstracts

1. Skopal J , Szigetfu E , Lakatos K , Gara E , Nardai S , Polos M , Nagy Z , Merkely B
   Optimalization of isolation and culture conditions of endothelial cells from human heart
   CARDIOVASCULAR RESEARCH 103:(Suppl. 1) Paper P184. (2014)
   3rd Congress of the ESC-Council-on-Basic-Cardiovascular-Science on Frontiers in Cardio Vascular Biology. Barcelona, Spanyolország: 2014.07.04 -2014.07.06.

2. Ruzsa Z , Nemes B , Pinter L , Berta B , Toth K , Nardai S , Merkely B
   Randomized comparison of transradial and transfemoral approach for carotid artery stenting
   JOURNAL OF THE AMERICAN COLLEGE OF CARDIOLOGY 62:(18 (Suppl. 1)) pp. B153-B154. (2013)
   25th Annual Symposium on Transcatheter Cardiovascular Therapeutics (TCT). San Marino: 2013.10.27 -2013.10.01.

3. Berta B , Nardai S , Barczi G , Becker D , Geller L , Jambrik Z , Molnar L , Ruzsa Z , Szabo G , Merkely B
   Xience V registry - Study of Xience V Everolimus-eluting and Vision cobalt-chromium coronary stent
   EUROINTERVENTION 7:(Suppl M) Paper 46. (2011)

4. Nardai S , Szabó Gy , Berta B , Édes I , Ruzsa Z , Jambrik Z , Gellér L , Merkely B
   Safety and Efficacy of Radial Approach during Rotablation
   INTERVENTIONAL MEDICINE AND APPLIED SCIENCE 3:(3) p. 179. (2011)
   19th International Meeting of the Alpe Adria association of cardiology. Budapest, Magyarország: 2011.09.15 -2011.09.17.

5. Szabó Gy , Ruzsa Z , Jambrik Z , Berta B , Édes I , Nardai S , Becker D , Merkely B
   Effectiveness and Long Term Results of Rotational Atherectomy in Heavily Calcified Left Main Bifurcation Lesions: Hard Plaque Preparation and the One Stent Technique
   AMERICAN JOURNAL OF CARDIOLOGY 107:(8 (Suppl.)) p. 13A. (2011)
   16th Annual Symposium on Interventional Vascular Therapeutics Angio Plasty Summit-Transcatheter Cardiovascular Therapeutics Asia Pacific. Seoul, Dél-Korea: 2011.04.27 -2011.04.29.

6. Nardai S , Szabó Gy , Berta B , Édes I , Merkely B
   Rotablation, the last remaining option for AMI patients with heavily calcified coronary lesions
   EUROPEAN HEART JOURNAL SUPPLEMENTS 12:(F) pp. F25-F26. (2010)
   4th Official Congress of the Working Group on Acute Cardiac Care. Copenhagen, Dánia: 2010.10.16 -2010.10.18.

7. Vincze C , Pál G , Wappler E A , Nardai S , Nagy Z , Lovas G , Dobolyi A
   Transforming growth factor beta isoforms in intact rat brain and following middle cerebral artery occlusion
   In: IBRO International Workshop 2010 . Konferencia helye, ideje: Pécs , Magyarország , 2010.01.21 -2010.01.23. Paper P3-35.
   (Frontiers in Neuroscience) Conference Abstract: IBRO International Workshop 2010

8. Zima E , Kovács E , Jenei Zs , Bárány T , Molnár L , Szilágyi Sz , Osztheimer I , Nardai S , Gellér L , Merkely B
   New thermo- and hemodynamic-controlled active hypothermic intensive treatment of post-resuscitated patients at Semmelweis University Heart Center.
   JOURNAL FUR KARDIOLOGIE 17:(Suppl A) p. 33. (2010)

9. Dobolyi A , Vincze C , Wappler E , Nardai S , Nagy Z , Lovas G
   Distribution of mRNAs encoding transforming growth factor beta 1, 2 and 3 in the normal and ischemic rat brain
   In: Society for Neuroscience, 39th Annual Meeting, 2009 . Konferencia helye, ideje: Chicago , Amerikai Egyesült Államok , 2009.10.17 -2009.10.21. Paper 737.11/N16.

ACKNOWLEDGEMENTS

I would like to express my greatest gratitude to my consultant supervisor **Prof. Zoltán Nagy**, who has determined the directions of our research and taught me science. I also have to thank my other consultant, **Dr. Judit Skopál**, who helped tremendously with the daily management of our projects. I am thankful to all the participating researchers, especially **Dr. Árpád Dobolyi**, as his contribution was essential to complete our work. As a practicing clinical I am very thankful to clinical supervisors **Prof. Béla Merkely**, **Dr. Dávid Becker**, and **Dr. István Szikora** for supporting my research efforts. Above all, I am really grateful to my wife **Dr. Eleonóra Imrédi** for her unlimited support.

APPENDIX

National Institute of Health Stroke Scale

Proposed neurological evaluation algorithm to determine the stroke severity score based on the recommendations of the National Institute of Neurological Disorders.

Category	Score/description	
1.a. Level of consciousness responsiveness	0= Alert 1=Drowsy 2=Stuporous 3=Coma	
1.b. LOC questions (Month, age)	0=Answers both correctly 1=Answers one correctly 2=Incorrect	
1.c. LOC commands (Open/close eye, make fist/let go)	0=Obeys both correctly 1=Obeys one correctly 2=Incorrect	
2. Best gaze (Eye open – patient follows examiner's finger to face)	0=Normal 1=Partial gaze palsy 2=Forced deviation	
3. Visual fields (Introduce visual stimulus/threat to patient's visual field quadrants)	0=No visual loss 1=Partial hemianopia 2=Complete hemianopia 3=Complete	
5a. Motor arm – left **5b. Motor arm – right** (Elevate arm to 90° if patient is sitting, to 45° if supine)	0=No drift 1=Drift 2=Can't resist gravity 3=No effort against gravity 4=No movement x=Untestable (joint fusion/amput.)	Left Right
6a. Motor leg – left **6b. Motor leg – right** (Elevate leg to 30° with patient supine)	0=No drift 1=Drift 2=Can't resist gravity 3=No effort against gravity 4=No movement x=Untestable (joint fusion/amput.)	Left Right
7. Limb ataxia (Finger-nose, Heel down shin)	0=No ataxia 1=Persistent in one limb 2=Persistent in two limbs	
8. Sensory (Pin prick to face, arm, trunk, and leg-compare side to side)	0=Normal 1=Partial loss 3=Severe loss	
9. Best language (Name item, describe a picture and read sentences)	0=No aphasia 1=Mild to moderate aphasia 2=Severe aphasia 3=Mute	
10. Dysarthria (Evaluate speech clarity by patient repeating listed words.)	0=Normal articulation 1=Mild to moderate slurring of words 2=Near to unintelligible or worse x=Intubated or other physical barrier	
11. Extinction and inattention **(**Use information from prior testing to identify neglect or double simultaneous stimuli testing.)	0=No neglect 1=Partial neglect 2=Complete neglect	